

Life-course neighbourhood deprivation and brain structure in older adults:

The Lothian Birth Cohort 1936

Gergő Baranyi¹, Colin R. Buchanan^{2,3}, Eleanor L.S. Conole², Ellen V. Backhouse^{4,6}, Susana Muñoz Maniega^{2,3,4,5,6}, Maria Valdes Hernandez^{2,3,4,5,6}, Mark E. Bastin^{2,3,4,5}, Joanna Wardlaw^{2,3,4,5,6}, Ian J. Deary², Simon R. Cox^{2,3}, Jamie Pearce¹

¹Centre for Research on Environment, Society and Health, School of GeoSciences, The University of Edinburgh, Edinburgh, UK.

²Lothian Birth Cohorts, Department of Psychology, The University of Edinburgh, Edinburgh, UK.

³Scottish Imaging Network, A Platform for Scientific Excellence (SINAPSE) Collaboration, Edinburgh, UK.

⁴Centre for Clinical Brain Sciences (CCBS), The University of Edinburgh, Edinburgh, UK.

⁵Edinburgh Imaging, The University of Edinburgh, Edinburgh, UK.

⁶UK Dementia Research Institute Centre at the University of Edinburgh, Edinburgh UK

*Corresponding author: Dr. Gergő Baranyi, Centre for Research on Environment, Society and Health, School of GeoSciences, University of Edinburgh, Drummond Street, Edinburgh EH89XP, United Kingdom, e-mail: gergo.baranyi@ed.ac.uk

NOTE: This preprint reports new research that has not been certified by peer review and should not be used to guide clinical practice.

ABSTRACT

Neighbourhood disadvantage may be associated with brain health but the importance at different stages of the life course is poorly understood. Utilizing the Lothian Birth Cohort 1936, we explored the relationship between residential neighbourhood deprivation from birth to late adulthood, and global and regional neuroimaging measures at age 73. We found that residing in disadvantaged neighbourhoods in mid- to late adulthood was associated with smaller total brain ($\beta=-0.06$; $SE=0.02$; $n=390$) and grey matter volume ($\beta=-0.11$; $SE=0.03$; $n=390$), thinner cortex ($\beta=-0.15$; $SE=0.06$; $n=379$), and lower general white matter fractional anisotropy ($\beta=-0.19$; $SE=0.06$; $n=388$). Regional analysis identified affected focal cortical areas and specific white matter tracts. Among individuals belonging to lower occupational social classes, the brain-neighbourhood associations were stronger, with the impact of neighbourhood deprivation accumulating across the life course. Our findings suggest that living in deprived neighbourhoods is associated with adverse brain morphologies, with occupational social class adding to the vulnerability.

COMPETING INTERESTS

The authors declare no competing interests.

INTRODUCTION

In 2020, there were 727 million people aged 65 years and older globally, with their proportion in the world's population (9.3%) expected to grow¹. One out of six individuals will be over 65 by 2050¹ and approximately 10% of this population will likely experience dementia (153 million)². Non-pathological cognitive decline heralds dementia and is much more common in older individuals: self-experienced decline in cognitive functioning affects one in four cognitively non-impaired adults over the age of 60³. Age-related changes in the brain structure can provide biologically traceable objective markers of cognitive function, revealing how the brain ages, and offering an early indicator of cognitive decline⁴. Accumulated evidence shows modest positive associations between cognitive function and total brain volume as well as various metrics of grey and white matter micro- and macrostructures⁵, and these relationships explain a significant proportion of individual differences in cognitive function and cognitive decline, especially in older ages^{4,6}.

Later-life cognitive function and decline has been linked to various neighbourhood-level characteristics^{7,8}, and there is some research connecting markers of brain morphology derived from magnetic resonance imaging (MRI) to physical and social features of the residential environment. Available cross-sectional studies suggest that neighbourhood deprivation is associated with structural brain differences among older adults,⁹⁻¹² which may partly explain the link between neighbourhood and cognitive function¹⁰. Moreover, residing in deprived areas may be a social stressor, which can amplify the impact of environmental threats on cognitive function¹³. Our understanding is more limited when it comes to the association between neighbourhood conditions and cortical disconnection¹⁴, the deterioration of the brain's connective pathways, for example, by axonal demyelination¹⁵. In addition to volumetric changes, disruptions in the brain's white matter also contribute to later-life cognitive decline^{4,15}. Diffusion MRI (dMRI) can quantify water molecular diffusion in white matter

microstructure¹⁶. From the diffusion tensor model we can obtain commonly used indicators of white matter microstructure such as fractional anisotropy (i.e., directional coherence of water molecule diffusion), and mean diffusivity (i.e., magnitude of water molecule diffusion), which typically go down and up with age, respectively¹⁵.

From a methodological perspective, existing research on neighbourhood and brain health in late adulthood is limited by cross-sectional and short-term longitudinal study designs which are prone to bias and/or confounding. Fluid cognitive abilities start to decline after young adulthood¹⁷ and the prodromal phase of dementia can stretch over a decade until diagnosis¹⁸. It is plausible that declining cognitive function and/or preclinical cognitive impairment impacts moving to neighbourhoods with specific amenities leading to reverse causation¹⁹. In addition to the impact of health status on moving, there is a degree of continuity in people's residential context across their life course, with neighbourhood disadvantage earlier in life predicting neighbourhood context later^{7,20}, increasing the likelihood of erroneously identifying later-life exposures as more relevant. Applying the life-course approach (i.e. examining the long-term impact of social and physical exposures on later health and diseases risk²¹) has the potential to overcome methodological biases,⁷ and it has been applied to explore individual-level risk factors of brain health among older adults²². Still, reconstructing objectively measured historical neighbourhood context over several decades remains a challenge and is not often done^{19,23}.

The present life-course study investigates whether living in deprived neighbourhoods from birth onwards was associated with global and regional brain health among older adults. Neighbourhood deprivation was operationalised as objectively measured area-level social disadvantage and it was linked to the residential history of participants in the Lothian Birth Cohort 1936 (LBC1936). We tested four exposure models to explain individual differences in grey and white matter macro- and microstructure at age 73 years: exposure to neighbourhood

deprivation in childhood (0-19 years), in young adulthood (20-39 years), in mid- to late adulthood (40-69 years), and accumulated neighbourhood deprivation across the life course (0-69 years). Analyses were fitted with linear regression within the structural equation modelling framework applying full information maximum likelihood estimation, which allowed optimal model estimation using all available data (see details in Methods). Little is known about whether some population groups show stronger associations between neighbourhood deprivation and brain health; therefore, we explored effect modification by sex, apolipoprotein E (*APOE*) ϵ 4 allele status, and individual-level social disadvantage in childhood and adulthood.

RESULTS

There were 689 individuals with at least one global brain measure available, the total sample size slightly varied across the eight global brain outcomes (Table 1). The average age was 72.68 years at the time of MRI acquisition, 52.69% of participants were male and 29.66% were *APOE* ϵ 4 allele carriers. Individuals with socially advantaged family backgrounds remained more likely to be socially advantaged as adults ($\chi^2= 30.42$; $p<0.001$); 25.76% and 57.82% of the sample belonged to higher occupational social class in childhood and in adulthood, respectively (Table 1). Neighbourhood deprivation could be only linked to participants residing in Edinburgh: childhood, young adulthood, mid- to late adulthood, and accumulated neighbourhood deprivation scores were available for 316, 388, 400, and 285 participants, respectively. Average deprivation scores decreased across participants' lives (Table 1), but they remained positively intercorrelated ($r=0.26-0.57$) (Supplementary Table 1). Individuals living in more deprived neighbourhoods throughout their life-course were more likely to belong to lower occupational social classes in childhood and adulthood (suggesting social segregation by geography and restricted social mobility), had lower childhood IQ scores, and spent fewer years in full-time education (Supplementary Table 2).

Table 1: Characteristics of study participants included in the analyses.

Characteristics	Total number	Mean \pm SD / number (%)
Global brain measures, mean \pm SD ^a		
Total brain volume (cm ³)	658	988.97 \pm 89.44
Grey matter volume (cm ³)	658	471.56 \pm 44.71
Normal-appearing white matter volume (cm ³)	658	475.01 \pm 50.66
White matter hyperintensity volume (cm ³)	672	12.06 \pm 12.84
Surface area (cm ²)	636	1533.72 \pm 144.92
Mean cortical thickness (mm)	636	2.26 \pm 0.10
General fractional anisotropy (standardized unit) ^b	665	0 \pm 1
General mean diffusivity (standardized unit) ^b	665	0 \pm 1
Neighbourhood deprivation, mean \pm SD		
In childhood (age 0-19 years)	316	0.57 \pm 3.39
In young adulthood (age 20-39 years)	388	-0.85 \pm 2.80
In mid- to late adulthood (age 40-69 years)	400	-2.35 \pm 2.74
Accumulated (age 0-69 years)	285	-2.00 \pm 6.84
Intracranial volume (cm ³), mean \pm SD	680	1450.83 \pm 140.52
Age in years, mean \pm SD	689	72.68 \pm 0.73
Sex, number (%)	689	
Male		363 (52.69%)
Female		326 (47.31%)
Father's occupational social class, number (%)	629	
High (professional-managerial)		162 (25.76%)
Low (skilled, partly skilled, and unskilled)		467 (74.24%)
<i>APOE</i> ϵ 4 allele status, number (%)	654	
ϵ 4 carriers		194 (29.66%)
Not ϵ 4 carriers		460 (70.34%)
Childhood IQ, mean \pm SD	652	100.80 (15.30)
Years spent in education, mean \pm SD	689	10.80 (1.14)
Adult occupational social class, number (%)	678	
High (professional-managerial)		392 (57.82%)
Low (skilled, partly skilled, and unskilled)		286 (42.18%)
Stroke, number (%) ^c	684	93 (13.60%)
Smoking status, number (%)	689	
Current smoker		56 (8.13%)
Ex-smoker		310 (44.99%)
Never smoked		323 (46.88%)
BMI, mean \pm SD	689	27.92 \pm 4.49
Self-reported history of		
Cardiovascular diseases, number (%)	689	187 (27.14%)
Diabetes, number (%)	689	75 (10.89%)
Hypertension, number (%)	689	339 (49.20%)
Stroke, number (%)	689	48 (6.97%)

^a The total number of outcome observations defined the sample size of the analyses; specific associations were based on the number of pairwise complete observations for the respective covariate-outcome pairs.

^b Operationalised as latent variable; in this table we report predicted values (standardized unit).

^c Identified from MRI scans by a consultant neuroradiologist.

Global brain measures

In the age and sex, (and intracranial volume for macrostructural outcome measures) adjusted model (i.e., Model 1), mid- to late adulthood neighbourhood deprivation was negatively associated with total brain volume, grey matter volume, mean cortical thickness, and general fractional anisotropy (p -value corrected for false discovery rate [p_{FDR}] <0.05) (Table 2). These associations remained significant ($p_{FDR}<0.05$) after further controlling for relevant life-course confounders (i.e., Model 2): neighbourhood deprivation in mid- to late adulthood was linked to smaller total brain (standardized effect size [β]=-0.06; standard error [SE]=0.02; $p_{FDR}=0.01$; sample size [N]=658; pairwise complete observations [n]=390) and smaller grey matter volumes ($\beta=-0.11$; SE=0.03; $p_{FDR}=0.003$; $N=658$; $n=390$), thinner cortex ($\beta=-0.15$; SE=0.06; $p_{FDR}=0.02$; $N=636$, $n=379$), and lower general fractional anisotropy ($\beta=-0.19$; SE=0.06; $p_{FDR}=0.005$; $N=665$, $n=388$) (Table 2). Although there were some significant associations with young adulthood and accumulated neighbourhood deprivation, these did not survive FDR correction.

Table 2: Associations between life-course models of neighbourhood deprivation and global brain measures

	Model 1 ^a				Model 2 ^b			
	β	SE	p	p_{FDR}	β	SE	p	p_{FDR}
<i>Childhood neighbourhood deprivation (n=296 to 311)</i>								
Total brain volume	-0.03	0.02	0.16	0.70	-0.04	0.02	0.10	0.38
Grey matter volume	-0.04	0.03	0.18	0.70	-0.05	0.03	0.09	0.38
Normal-appearing white matter volume	0.01	0.03	0.76	0.87	0.02	0.03	0.61	0.81
White matter hyperintensity volume	-0.01	0.05	0.81	0.87	-0.03	0.05	0.58	0.81
Cortical surface area	-0.01	0.03	0.68	0.87	-0.01	0.03	0.84	0.95
Mean cortical thickness	-0.06	0.06	0.33	0.78	-0.07	0.06	0.25	0.56
General fractional anisotropy ^c	-0.05	0.06	0.39	0.78	-0.07	0.06	0.28	0.56
General mean diffusivity ^c	-0.01	0.06	0.87	0.87	0.00	0.06	0.96	0.95
<i>Young adulthood neighbourhood deprivation (n=367 to 383)</i>								
Total brain volume	-0.01	0.02	0.60	0.69	-0.02	0.02	0.36	0.41
Grey matter volume	-0.03	0.03	0.26	0.38	-0.05	0.03	0.12	0.22
Normal-appearing white matter volume	0.04	0.03	0.21	0.38	0.05	0.03	0.14	0.22
White matter hyperintensity volume	-0.01	0.05	0.82	0.82	-0.04	0.05	0.47	0.47
Cortical surface area	-0.04	0.03	0.17	0.38	-0.05	0.03	0.06	0.18
Mean cortical thickness	-0.14	0.05	0.01	0.06	-0.10	0.05	0.07	0.18
General fractional anisotropy ^c	-0.12	0.06	0.04	0.15	-0.14	0.06	0.02	0.15
General mean diffusivity ^c	-0.06	0.06	0.28	0.38	-0.06	0.06	0.35	0.41
<i>Mid- to late adulthood neighbourhood deprivation (n=379 to 396)</i>								
Total brain volume	-0.05	0.02	0.010	0.02	-0.06	0.02	0.004	0.01
Grey matter volume	-0.09	0.03	0.003	0.01	-0.11	0.03	<0.001	0.003
Normal-appearing white matter volume	-0.06	0.03	0.05	0.08	-0.07	0.03	0.03	0.05
White matter hyperintensity volume	0.04	0.05	0.39	0.45	0.05	0.05	0.35	0.40
Cortical surface area	-0.03	0.03	0.22	0.29	-0.04	0.03	0.16	0.22
Mean cortical thickness	-0.19	0.05	<0.001	0.002	-0.15	0.06	0.01	0.02
General fractional anisotropy ^c	-0.14	0.05	0.008	0.02	-0.19	0.06	0.001	0.006
General mean diffusivity ^c	-0.02	0.06	0.70	0.70	0.03	0.06	0.68	0.68
<i>Accumulated neighbourhood deprivation (n=268 to 281)</i>								
Total brain volume	-0.04	0.02	0.05	0.16	-0.05	0.03	0.03	0.13
Grey matter volume	-0.06	0.03	0.06	0.16	-0.09	0.04	0.01	0.11
Normal-appearing white matter volume	0.00	0.03	0.98	0.98	0.02	0.04	0.69	0.69
White matter hyperintensity volume	0.00	0.05	0.93	0.98	-0.03	0.06	0.62	0.69
Cortical surface area	-0.03	0.03	0.34	0.46	-0.03	0.04	0.50	0.67
Mean cortical thickness	-0.16	0.06	0.01	0.09	-0.11	0.07	0.13	0.27
General fractional anisotropy ^c	-0.08	0.06	0.19	0.38	-0.14	0.07	0.06	0.17
General mean diffusivity ^c	-0.07	0.07	0.28	0.45	-0.06	0.08	0.44	0.67

Models were fitted within the structural equation modelling framework applying full information maximum likelihood estimation. Total sample size was $N=658$ for total brain, grey matter and normal-appearing white matter volumes, $N=672$ for white matter hyperintensity volume, $N=636$ for cortical surface area and mean cortical thickness, and $N=665$ for general fractional anisotropy and mean diffusivity. Information on the numbers of complete exposure-outcome observations (n) is presented in Supplementary Table 3; model fit indices for general fractional anisotropy and general mean diffusivity are in Supplementary Table 4 (all other models were fully saturated). Bold typeface denotes false discovery rate adjusted significance (p_{FDR}). SE = standard error.

^a Models were adjusted for sex and age (and intracranial volume for macrostructural measures).

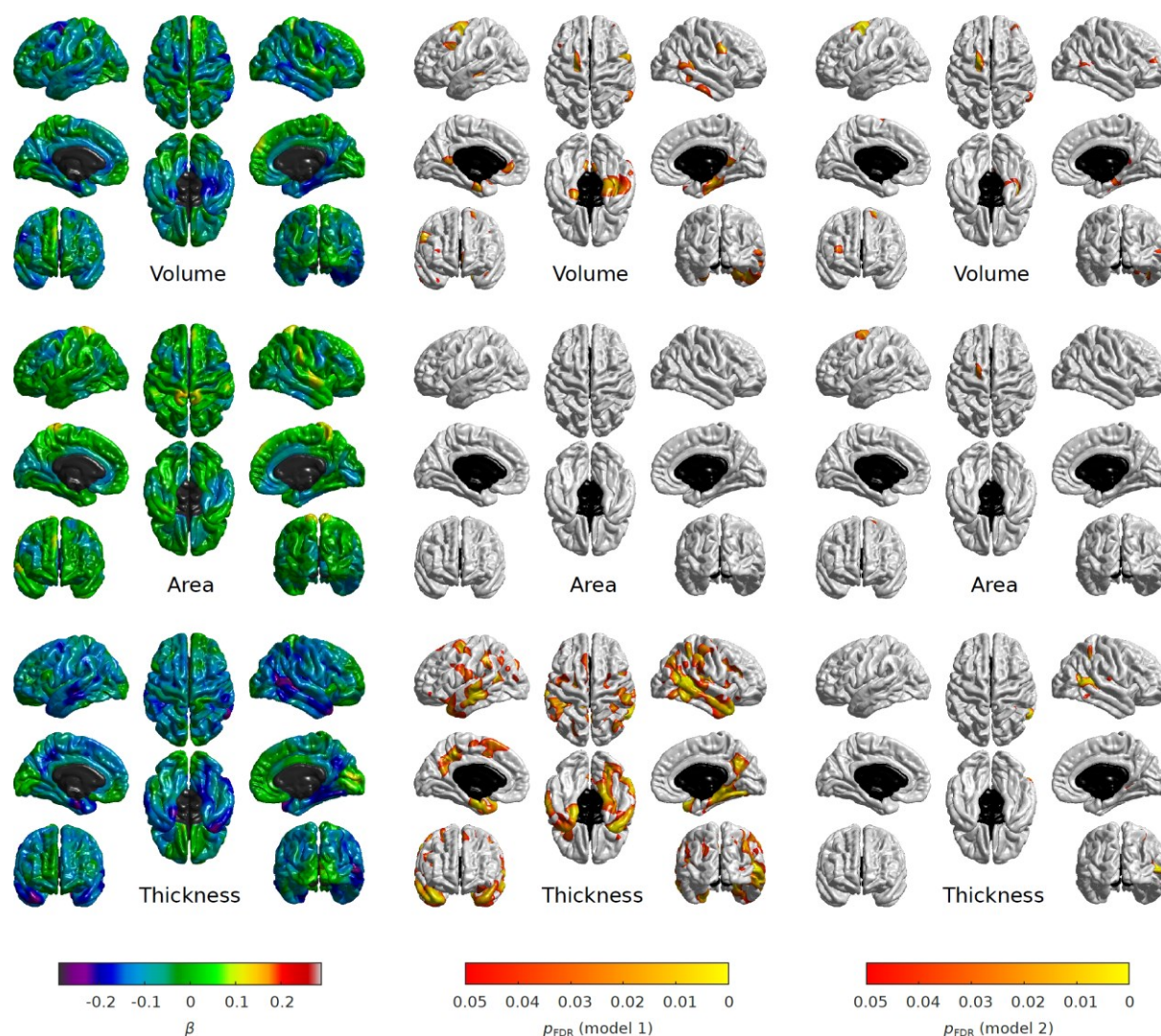
^b Models were adjusted for sex, age, (intracranial volume for macrostructural measures,) father's occupational social class and *APOE* $\epsilon 4$ allele status. In addition, young adulthood models were adjusted for childhood IQ and years spent in education, and mid- to late adulthood/ accumulation models also for adult occupational social class.

^c No adjustment for intracranial volume.

Local brain measures: vertex-wide analysis

We explored regional associations across the entire cortical surface using vertex-wise analysis. After applying Model 1 adjustment, greater young adulthood and greater mid- to late adulthood neighbourhood deprivation was associated with lower cortical volume, and a thinner cortex, while greater accumulated neighbourhood deprivation was associated with a thinner cortex (Supplementary Figure S1-3). After further controlling for relevant life-course confounders (Model 2) only mid- to late adulthood neighbourhood deprivation associations remained FDR-corrected significant (Supplementary Figure S4-6; Figure 1). Specifically, greater mid- to late adulthood neighbourhood deprivation (N=622; n=371) was associated with lower cortical volume (mean β =-0.05; β range: -0.27 to 0.14); smaller cortical surface area (mean β =-0.02; β range: -0.22 to 0.15); and a thinner cortex (mean β =-0.08; β range: -0.28 to 0.12). There was a spatial overlap in the areas identified across the three cortical measures, particularly between volume and area (Dice coefficient=0.33), and between volume and thickness (Dice coefficient=0.13). The significant regions were in the: posterior area of the left superior frontal gyrus (both volume and area); rostral area of the right middle frontal gyrus (volume); right parahippocampal cortex (volume); right isthmus cingulate cortex (volume); caudal area of the right middle temporal gyrus (volume and thickness); caudal area of the right inferior temporal gyrus (thickness); and a lateral area of the right superior parietal lobule (thickness) (Figure 1).

Figure 1: Regional associations between mid- to late adulthood neighbourhood deprivation and cortical properties (volume, surface area, and thickness). The fully adjusted standardized coefficients were obtained in linear regression models fitted within the structural equation modelling framework applying full information maximum likelihood estimation. Sample size was $N=622$, pairwise complete observations were $n=371$. The heatmaps show (left to right): standardised betas (Model 1), FDR-adjusted p -values for Model 1 ($p_{FDR}<0.05$) and FDR-adjusted p -values for Model 2 ($p_{FDR}<0.05$); the non-cortical mask is shown in black.

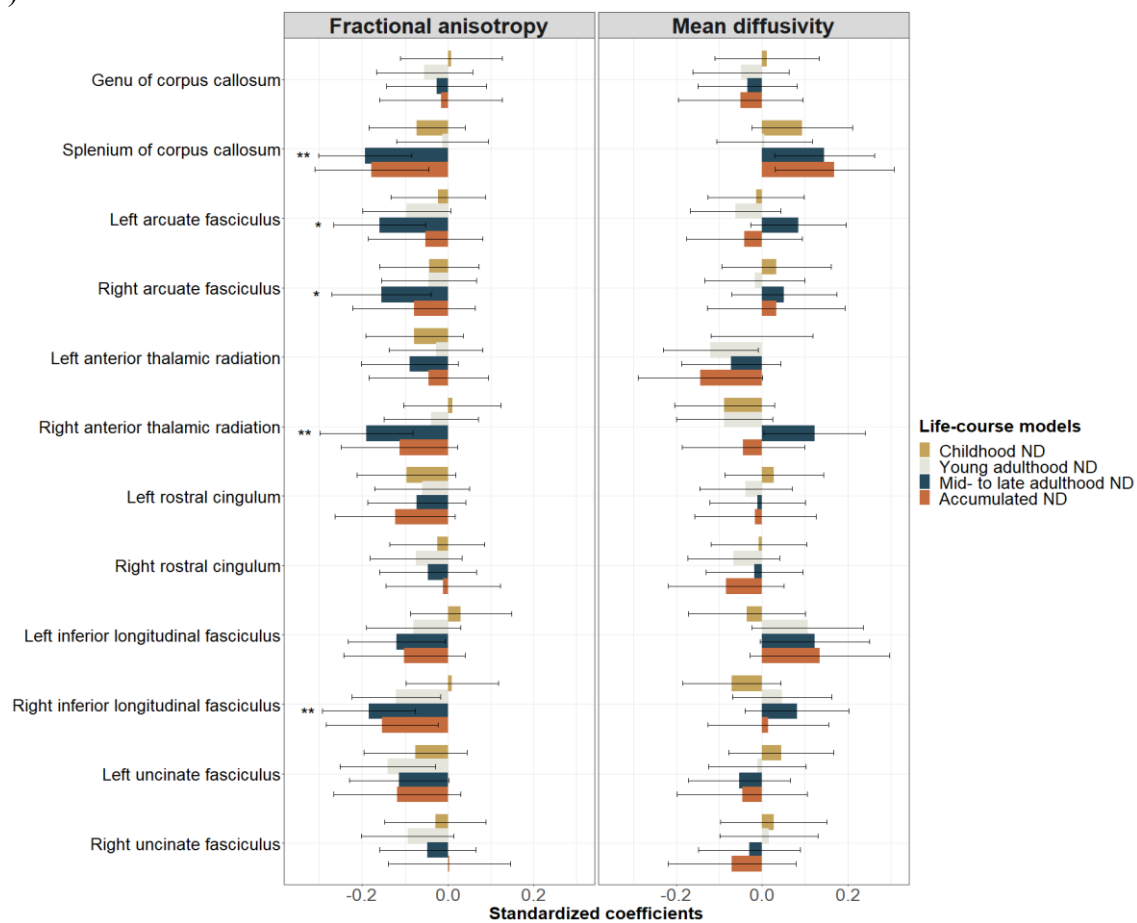


Local brain measures: white matter tracts

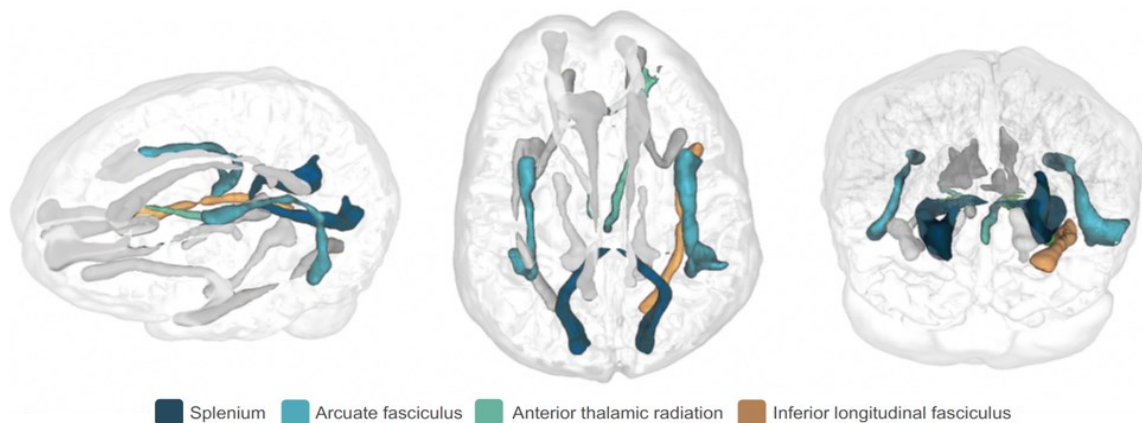
Associations with neighbourhood deprivation were investigated in each of the twelve white matter tracts (Supplementary Figure 7). After FDR-correction, higher mid- to late adulthood neighbourhood deprivation was associated with lower fractional anisotropy in four tracts, in both Model 1 (Supplementary Table 5) and Model 2 (Supplementary Table 6): splenium of corpus callosum (Model 2: $\beta=-0.19$; SE=0.06; $p_{FDR}=0.003$; $N=652$; $n=379$), right anterior thalamic radiation (Model 2: $\beta=-0.19$; SE=0.06; $p_{FDR}=0.003$; $N=662$; $n=371$), right inferior longitudinal fasciculus (Model 2: $\beta=-0.18$; SE=0.06; $p_{FDR}=0.003$; $N=663$; $n=386$), and left arcuate fasciculus (Model 2: $\beta=-0.16$; SE=0.06; $p_{FDR}=0.01$; $N=655$; $n=381$). Right arcuate fasciculus became FDR-significant in Model 2 ($\beta=-0.16$; SE=0.06; $p_{FDR}=0.02$; $N=621$; $n=360$) (Figure 2). Although there were no significant findings for mean diffusivity, stronger opposite direction associations in the same white matter tracts (e.g., splenium) reinforced findings for fractional anisotropy.

Figure 2: Association between life-course models of neighbourhood deprivation, and fractional anisotropy and mean diffusivity in twelve white matter tracts (A), and the location of false discovery rate (FDR)-adjusted significant tracts within the brain of a participant (B). Standardized coefficients with their 95% CI were obtained in linear regression models fitted within the structural equation modelling framework applying full information maximum likelihood estimation. Models were adjusted for sex, age, intracranial volume, father’s occupational social class, APOE ϵ 4 allele status. In addition, young adulthood models were adjusted for childhood IQ and years spent in education, and mid- to late adulthood/accumulation models also for adult occupational social class. Asterisks denote FDR-adjusted significance ($*p_{FDR}<0.05$; $**p_{FDR}<0.01$). ND=neighbourhood deprivation.

(A)



(B)

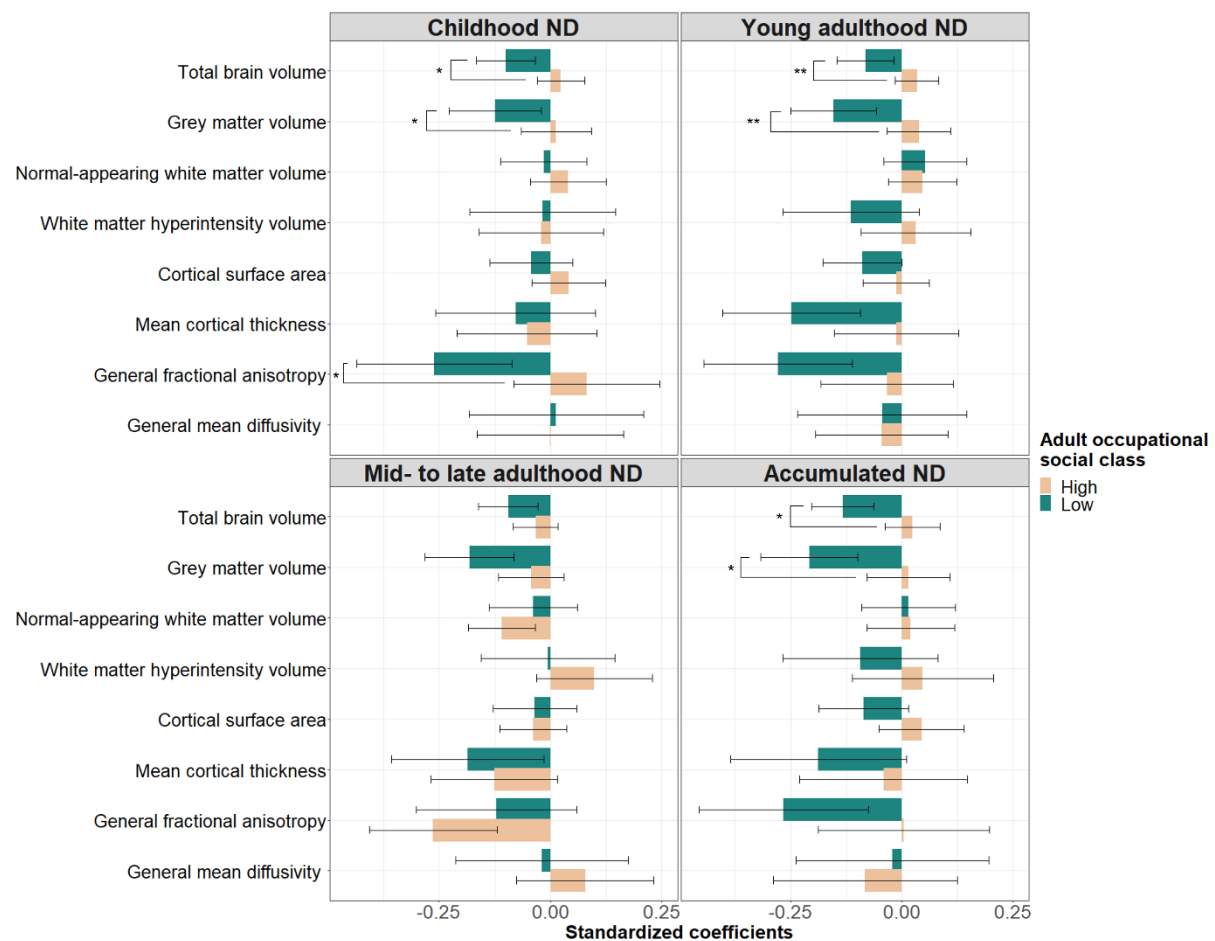


Social class modifies neighbourhood-brain associations

We explored effect modification by age, *APOE* $\epsilon 4$ allele status, and occupational social class in childhood and adulthood. No FDR-adjusted differences were detected between females and males, or between $\epsilon 4$ carriers and non- $\epsilon 4$ carriers (Supplementary Table 7). The associations between neighbourhood deprivation and brain structural differences were stronger among individuals belonging to lower occupational social classes in childhood and in adulthood (i.e., skilled, partly skilled, and unskilled). Growing up in relatively disadvantaged households meant stronger negative association between young adulthood neighbourhood deprivation and late adulthood cortical surface area ($\beta=-0.12$; $SE=0.04$; $p_{FDR}=0.007$; $N=433$; $n=255$) in comparison to higher social class households (i.e., professional-managerial).

Effect modification was found by own adult social class. Among individuals belonging to lower occupational social classes, higher childhood, young adulthood, and accumulated neighbourhood deprivation negatively associated with total brain and grey matter volumes, and – for childhood exposure – with general fractional anisotropy (Supplementary Table 7). When we estimated the associations of accumulated neighbourhood deprivation with total brain ($\beta=-0.13$; $SE=0.04$; $p_{FDR}=0.001$; $N=272$; $n=126$) and grey matter volumes ($\beta=-0.21$; $SE=0.06$; $p_{FDR}=0.001$; $N=272$; $n=126$) among socially disadvantaged individuals, these were 30.0% and 16.7% larger in magnitude, compared to any other life-course models (Supplementary Table 8). Figure 3 depicts associations between life-course models of neighbourhood deprivation and global brain measures by adult occupational social class.

Figure 3: Association between life-course models of neighbourhood deprivation and global brain measures among participants belonging to high (i.e., professional-managerial) and low (i.e., skilled, partly skilled, and unskilled) occupational social classes in adulthood. Standardized coefficients with their 95% CI were obtained in linear regression models fitted within the structural equation modelling framework applying full information maximum likelihood estimation. Models were adjusted for sex, age, intracranial volume, father’s occupational social class, and APOE $\epsilon 4$ allele status; in addition, young adulthood/ mid- to late adulthood/ accumulation models were adjusted for childhood IQ and years spent in education. Asterisks denote FDR-adjusted significant interactions ($*p_{FDR}<0.05$; $**p_{FDR}<0.01$). ND=neighbourhood deprivation.



Sensitivity analyses

After regressing young adulthood on childhood neighbourhood deprivation scores, effect sizes for the global brain measures dropped in magnitude with an average of 17%. After regressing mid- to late adulthood on young adulthood scores, associations were on average 15% lower; still, findings remained comparable (Supplementary Table 9). Adjusting for stroke identified from MRI scans did not affect the results (Supplementary Table 10). Controlling mid- to late adulthood exposure for health-related variables (i.e., BMI, smoking, self-reported medical diagnosis of chronic diseases) yielded 20% reduction of effect sizes on average, but findings remained comparable with the exemption of mean cortical thickness (-33%) (Supplementary Table 11). Applying a strict criterion with valid deprivation scores for each decade of the respective life-course model, reinforced the main findings. Importantly, it also suggested that accumulated neighbourhood deprivation significantly contributes to total brain volume ($\beta=-0.09$; $SE=0.03$; $p_{FDR}=0.03$; $N=658$; $n=222$) with an effect size of 50% larger than for mid- to late adulthood exposure (Supplementary Table 12). When we excluded individuals from the sample with any signs of cognitive impairment, associations remained comparable with young adulthood exposure and general fractional anisotropy, as well as accumulated deprivation and total brain volume becoming FDR-significant (Supplementary Table 13). Finally, utilising linear regression with complete case analysis decreased power, but led to comparable nominal associations as the main analyses with general fractional anisotropy remaining (FDR-adjusted) significantly associated with neighbourhood deprivation in young adulthood and in mid-to-late adulthood (Supplementary Table 14).

DISCUSSION

This study demonstrates that living in disadvantaged neighbourhoods across the life course is linked to brain structural differences among older adults. First, mid- to late adulthood

neighbourhood deprivation was modestly associated with global and regional brain morphology. Participants living in deprived neighbourhoods had smaller total brain and grey matter volumes, thinner cortex, and lower general fractional anisotropy. Cortical differences were identified in both hemispheres, mainly in the left superior frontal gyrus and the right middle temporal gyrus. Smaller areas of significance were in right inferior frontal gyrus, right parahippocampal cortex, right cingulate cortex, right middle temporal gyrus, and the right superior parietal lobule. Regional associations for white matter tracts included lower fractional anisotropy in the splenium, in the arcuate fasciculus, in the right anterior thalamic radiation, and in the right inferior longitudinal fasciculus. Second, individual social disadvantage across the life-course amplified the association of neighbourhood deprivation with brain structural differences. Participants growing up in disadvantaged households showed additional detrimental impacts of neighbourhood deprivation in young adulthood, materialising as smaller cortical surface area. Participants belonging to lower occupational social classes in adulthood showed more accumulated impact of neighbourhood deprivation on total brain and grey matter volume. Sensitivity analyses reinforced the main associations with mid- to late adulthood neighbourhood deprivation, especially for grey matter volume and general fractional anisotropy.

The brain's macro and micro-structure is constantly changing across the human life course. Total brain volume, for example, increases throughout childhood and adolescence, and after a plateau in young adulthood, a steady volume loss occurs with further acceleration after the age of 60 years^{24,25}. Neighbourhood deprivation may have long-term impacts on brain morphology, where aspects of social and environmental change may disrupt aspects of brain development during critical periods. Our study suggests that exposure to higher neighbourhood disadvantage in mid- to late adulthood (age 40-69), a period characterised with brain degeneration^{24,25}, was linked to brain structural differences (i.e., reduced total brain and grey matter volume, thinner

cortex and lower general fractional anisotropy). Available cross-sectional evidence supports these findings^{9-12,14,26}. Living in disadvantaged areas is associated with smaller total brain volume⁹, and with cortical thinning in Alzheimer's disease signature regions¹⁰ in older age, but not with white matter hyperintensities¹¹ – in line with our findings. Comparable associations were found in midlife for global brain outcomes¹², for surface area and cortical thickness in regions linked to language and executive functions²⁶, as well as for white matter fractional anisotropy¹⁴. The specific cortical regions we identified overlap with Alzheimer-relevant areas and are thought to be involved in executive function and perception (left superior frontal), emotion (right middle temporal and right isthmus cingulate), social cognition and working memory (right middle frontal), and imagination and perception (right superior parietal lobule); the identified white matter tracts are potentially involved in production and understanding of language (arcuate fasciculus), executive function (anterior thalamic radiation), and visual and semantic processing (inferior longitudinal fasciculus).²⁷ However, further studies are required to confirm regional associations.

Individual social disadvantage across the life course modified the relationship between neighbourhood deprivation and brain morphology, whereas there were no effect modifications by sex and *APOE* $\epsilon 4$ allele status (in line with previous studies on neighbourhood exposures^{9,28}). Interaction between family and neighbourhood disadvantage in childhood has been observed in cross-sectional studies; children from disadvantaged families living in more deprived areas have lower cortical thickness²⁹, and stronger age-related decrease in cortical thickness³⁰ in comparison to children from advantaged families. Increasing evidence shows that material disadvantage not only associates with brain structure during later-life, but also during childhood and adolescence³¹, with early life factors having long-term consequences likely lasting throughout life^{22,32}. Cross-sectional studies found smaller global and regional cortical surface area³³, smaller cortical³⁴ and subcortical volumes³³, and lower cortical

thickness^{29,30} among children exposed to greater neighbourhood deprivation. Social disadvantage (including area deprivation) also contributes to lower white matter integrity among newborns^{35,36} and children³⁷. Importantly, childhood neighbourhood deprivation can have long-term consequences for brain development with longitudinal studies showing lower white matter quantitative anisotropy³⁸ and greater amygdala reactivity³⁹ in younger adulthood. Our study adds a life course perspective to these findings, but also extends previous LBC1936 analysis finding null associations between father's occupational social class and total brain volume²²: multi-faced disadvantage (individual and area-level) in early life was associated with cortical surface area differences among older adults.

The more time individuals spent living in deprived neighbourhoods across their lives, the larger were the association between neighbourhood deprivation and brain structural differences; these findings were particularly marked for disadvantaged adults. Possibly, through the accumulation model, we may have captured area-level processes affecting the brain's morphology both during its development in childhood and during its degeneration in mid- to late adulthood, and individuals with lower personal resources across the life course, including cognitive reserve⁴⁰, were more vulnerable. Alternatively, it is also plausible that in our study accumulated neighbourhood deprivation only affected the brain during its degeneration phase (e.g., through cumulative allostatic load⁴¹), with the lagged impact of early life neighbourhood deprivation 'kicking in' in later adulthood. However, in the absence of neuroimaging data and area-level deprivation measured across the entire life course within the same individuals, these hypotheses cannot be verified and only present associations without causal implications. As such data are likely many years away from being feasible, future studies should apply pseudo-/ accelerated longitudinal designs in different age groups to further explore the reported interactions.

Residing in disadvantaged areas might influence brain morphology through multiple interrelated ways and the underlying processes may differ across the life course.

Socioeconomically disadvantaged areas are likely to suffer from poorer housing conditions⁴², higher crime and violence⁴³, have lower provision of high quality green space⁴⁴, and residents are more likely to be exposed to higher levels of contaminants (e.g. air pollution⁴⁵), poorer diet, and to health-damaging commodities and services, such as alcohol, fast food and tobacco outlets⁴⁶; these, in turn, can associate with brain morphology and function (e.g. green space²⁸, air pollution⁴⁷). In childhood, the quality of local schools, in late adulthood the availability of neighbourhood resources and amenities (e.g., community and cultural centres), may be pertinent. Neighbourhood disadvantage may contribute to brain structural differences through multiple interrelated pathways. Research shows that children exposed to stressors in their social environment experience activated hypothalamic-pituitary-adrenal axis which leads to long-term dysregulation and changes in the brain^{31,39}. Investigated pathways in adulthood include inflammatory^{14,26}, neuroendocrine¹² and cardiovascular⁹ mechanisms.

We describe associations between neighbourhood deprivation from birth to late adulthood and global and regional brain differences. Study strengths included the narrow age-range and homogeneity of participants, the availability of residential history and objectively measured neighbourhood disadvantage covering an exceptionally long period of ~70 years, the detailed assessment of global and regional brain measures, and the availability of key life-course social, biological, and psychological confounders (e.g., father's social class, *APOE* ϵ 4 allele status, childhood IQ). There are limitations to acknowledge. First, our sample consisted of a relatively healthy, educated and urbanised group of older adults, with higher childhood IQ⁴⁸ and lower risk of mortality⁴⁹ in comparison to the population average, leading to selection and survival bias. Second, given the challenges of collecting objective neighbourhood data across the life course (i.e., deprivation scores could be obtained only for individuals residing in Edinburgh) our effective sample was moderate (ranging from 268 to 396), and it differed across the four life-course models. It is plausible that analyses for specific models were relatively

underpowered in comparison to others; still, restricting the sample size to participants with observations available for all four models would have led to significant drop in relevant observations (>30%), increased type II error, and sample bias. Third, reconstructing neighbourhood deprivation indices across the 20th century was challenged by the inconsistent availability of historical data and their varying spatial aggregation in official records. Although 1961 ward geographies likely do not align with participant's self-defined neighbourhoods, they were necessary to provide a common spatial resolution to handle missing data²³. Fourth, information on health status prior to late adulthood is not available in LBC1936, which likely increases the risk of unmeasured confounding through selective residential mobility. Fifth, MRI data was only available in late adulthood; therefore, we cannot ascertain whether there is a direct pathway between childhood area disadvantage and later-life brain outcomes, or childhood exposure first influenced childhood brain development. Last, we tested a large number of associations and, to reduce type 1 error rate, we highlighted only FDR-adjusted significant results. It is plausible that we missed important associations.

Future studies could usefully replicate our findings in larger and more socially and ethnically diverse samples with repeatedly measured neighbourhood exposures and brain outcomes across the life course, and with specific focus on downward and upward social and geographic mobility. Furthermore, testing life-course associations for subcortical structures, identifying specific neighbourhood features most likely contributing to brain health, systematically assessing causal pathways over the lifespan (e.g., hypothalamic-pituitary-adrenal axis, inflammation, cardiovascular risks), and understanding the double burden of disadvantaged people living in disadvantaged areas requires further attention.

Conclusions

Living in deprived neighbourhoods across the life course was associated with worse brain health among older adults, which can be measured over and above individual-level differences. Neighbourhood deprivation during later-life (age 40-69 years) was associated with brain structural differences in older age, but we also found some evidence for the accumulating impact of neighbourhood deprivation across the entire life course, especially among socially disadvantaged individuals. The life course approach can provide useful insights into how the social environment might ‘get under the skin,’ and future research should apply it more often to understand differences and changes in brain morphology and related cognition. Greater understanding of relevant brain regions, social and physical neighbourhood features pertinent to brain health, and potential causal pathways require further research attention.

METHODS

Study participants

Data were drawn from the LBC1936, a longitudinal study of relatively healthy older adults born in 1936. LBC1936 was designed to follow up some participants of the Scottish Mental Survey 1947 – a nationwide general cognitive testing exercise carried out among all 1936-born children attending Scottish schools on June 4th, 1947 – with the main aim to study non-pathological cognitive ageing in later life^{50,51}. Surviving participants of the Scottish Mental Survey 1947 living in the City of Edinburgh and the surrounding Lothian region of Scotland were traced and contacted by the Lothian Health Board⁵¹. Between 2004 and 2007 (Wave 1; mean age=70 years), 1091 subjects underwent detailed social, cognitive and health assessments; since Wave 2 (2007-2010; mean age=73 years; $n=866$), neuroimaging data are also available⁵¹. In 2014 (mean age=78 years), a ‘life grid’ questionnaire was administered among surviving LBC1936 participants to collect retrospective account of their residential

history for every decades from birth to date of completion⁵⁰. Flashbulb memory prompts (e.g. 9/11 attacks in New York) and participant supplied personal events assisted recall²³. 593 cohort members provided life-course addresses (84% completion rate) which were geocoded using automatic geocoders and historical building databases²³.

Neighbourhood deprivation

Life-course neighbourhood deprivation was operationalised as small area-level social disadvantage, computed for the City of Edinburgh once for every decades of the study with data derived from administrative records²³. In 1941, 1951, 1961 and 1971, information on overcrowding, population density, infant mortality, tenure and amenities contributed to an index of multiple deprivation²³; for 1981, 1991 and 2001, we utilised the Carstairs index of deprivation (i.e. male unemployment, overcrowding, car ownership, low social class)⁵². Geographic data were aggregated to a common spatial resolution (1961 ward-level; $n=23$) in order to support estimating of missing indicators; z -scores were calculated to ensure comparability across the two indices²³. We linked residential addresses to deprivation scores using 10-year intervals (e.g., 1941 score linked to 1936-1945 addresses). Exposures closer in time were highly correlated ($r>0.61$) (Supplementary Figure 8). Finally, three periods captured average exposures to neighbourhood deprivation during childhood (1936-1955), young adulthood (1956-1975) and mid- to late adulthood (1976-2005) for participants having any valid exposure data during these epochs⁵³. Accumulated neighbourhood disadvantage was calculated as the mean exposure across the three periods, requiring valid measurement of neighbourhood deprivation (i.e., living in the City of Edinburgh) at least once for each.

MRI acquisition

All brain data were acquired between 2007 and 2010 (Wave 2); the MRI acquisition parameters have been described previously⁵⁴. All participants underwent brain MRI on a 1.5 T GE Signa

Horizon HDx clinical scanner (General Electric, Milwaukee, WI) with a manufacturer supplied 8-channel phased-array head coil. High resolution 3D T₁-weighted inversion-recovery prepared, fast spoiled gradient-echo volumes were acquired in the coronal plane with 160 contiguous 1.3 mm thick slices resulting in voxel dimensions of 1 × 1 × 1.3 mm. T₂-weighted fast spin echo volumes were acquired in the coronal plane with 80 contiguous 2 mm thick slices resulting in voxel dimensions of 1 × 1 × 2 mm. For the dMRI protocol, single-shot spin-echo echo-planar (EP) diffusion-weighted whole-brain volumes ($b=1000 \text{ s mm}^{-2}$) were acquired in 64 noncollinear directions, along with seven T₂-weighted volumes ($b=0 \text{ s mm}^{-2}$). Seventy-two contiguous axial 2 mm thick slices were acquired resulting in 2 mm isotropic voxels.

Image processing

We assessed both global and regional brain measures. From the T₁- and T₂-weighted data, various tissue volumes were estimated as described previously⁵⁴. Total brain volume was estimated as intracranial volume minus cerebrospinal fluid, and grey matter volume as total brain volume minus white matter volume. White matter volume was segmented into normal appearing-white matter and white matter hyperintensities, the latter defined as hyperintense areas (>3 mm in diameter) in white matter. Additionally, cortical reconstruction was performed with the FreeSurfer image analysis suite (<http://surfer.nmr.mgh.harvard.edu>) v5.1.0. Cortical surface analyses were then performed using the SurfStat MATLAB toolbox (<http://www.math.mcgill.ca/keith/surfstat>). Surfaces were aligned vertex-wise into a common space (the FreeSurfer average template) and spatially smoothed at 20 mm full width at half maximum, allowing sample-wide analyses of volume, area, and thickness across the cortex.

All raw dMRI data were converted from DICOM to NIfTI-1 format using TractoR v2.6.2⁵⁵. Using tools freely available in the FSL toolkit v4.1.9 (FMRIB, Oxford University: <http://www.fmrib.ox.ac.uk>)⁵⁶, data underwent brain extraction⁵⁷ performed on the T₂-weighted

EP volumes acquired along with the dMRI data. The brain mask was applied to all volumes after correcting for systematic eddy-current induced imaging distortions and bulk patient motion using affine registration to the first T₂-weighted EP volume of each participant⁵⁸. For all dMRI volumes, diffusion tensors were fitted at each voxel and water diffusion measures were estimated for mean diffusivity and fractional anisotropy at each voxel. Tractography was performed using an established probabilistic algorithm with a two-fibre model per voxel (BEDPOSTX/ProbtrackX)^{59,60}. Analysis of twelve major white matter tracts was performed using probabilistic neighbourhood tractography⁵⁵. These tracts were the genu and splenium of the corpus callosum, left and right arcuate fasciculi, left and right anterior thalamic radiation, left and right rostral cingulum, left and right inferior longitudinal fasciculus, and left and right uncinate fasciculus (see Supplementary Figure 7 for their locations). All tracts were visually quality checked, and exclusions were made on a tract basis. Tract-averaged diffusion parameters (i.e., fractional anisotropy, mean diffusivity) weighted by the streamline visitation count were then calculated from all voxels by tract^{54,61}.

Covariates

Relevant confounders were selected based on the literature^{7,9} and are presented in a directed acyclic graph (Supplementary Figure 9). Age and sex (female, male) were included in all presented models. *APOE* ϵ 4 allele status (ϵ 4 carriers, not ϵ 4 carriers) is a genetic risk factor of cognitive decline⁶². Father's occupational social class was classified into high (I/II: professional-managerial) and low classes (III/IV/V: skilled, partly skilled and unskilled)⁶³; the same categorisation was used for own social class in adulthood (for women, husband's class was taken if higher). Childhood IQ was measured at age 11 years with the Moray House Test No 12⁵⁰, and education was captured as years spent in full-time education. In sensitivity analyses, we considered a range of health-related variables, which can be theorised as confounders, but also as mediators between neighbourhood deprivation and brain health⁷. They

were collected at the time of MRI acquisition (i.e., Wave 2) and included stroke identified from MRI scans by a consultant neuroradiologist (yes, no), body mass index (BMI), smoking status (current smoker, past smoker, never smoked), and self-reported medical diagnosis (yes, no) of stroke, diabetes, hypertension, and cardiovascular disease.

Statistical analysis

Models were fitted with full-information maximum likelihood (FIML) estimation within structural equation modelling (SEM) using the *lavaan* package⁶⁴ v0.6-12 in R v4.2.1⁶⁵. FIML regression has the advantage of estimating model parameters based on all available information, including participant with missing variables, increasing power, and thus lowering type II error. Importantly, fitting models in the context of all available data for confounders enables to calculate model residuals in a larger and more comprehensive sample and to estimate the impact of exposure more accurately. FIML regression produces equivalent results to models handling missing data with multiple imputation⁶⁶. We reported total sample size for each analysis (N) and the number of pairwise complete observations (n) for associations of interest. Goodness of fit indices were not provided for fully saturated models.

The primary analysis tested the associations between neighbourhood deprivation scores and global brain measures, including six macro-structural outcomes (total brain, grey matter, normal-appearing white matter, and white matter hyperintensity [log-transformed to approximate normal distribution⁶¹] volumes, cortical surface area, and mean cortical thickness) and two markers of white matter microstructure. Consistent with prior work⁶⁷, general factors of fractional anisotropy and mean diffusivity across the twelve white matter tracts were estimated as latent factors; we included residual correlations between the splenium and the genu of corpus callosum, and between right and left sides of the bilateral tracts (see

Supplementary Table 15 for fit indices and factor loadings). We provided p_{FDR} correcting for multiple comparison⁶⁸ between the eight global brain outcomes.

Local brain associations were explored in the secondary analyses. We estimated regional associations with life-course neighbourhood deprivation across the entire cortical surface. Vertex-wise analysis was performed in a common space (the FreeSurfer average template) for 327,684 cortical vertices using all MRI participants with cortical surface data. Three vertex-wise brain measures were assessed: cortical volume, surface area and thickness. Vertex measures were exported from SurfStat and then SEM with FIML was used to iteratively estimate standardised coefficients and the corresponding p -values by vertex for each neighbourhood deprivation exposure. Correction for multiple comparison was performed by FDR and the findings were presented in cortical surface maps. The spatial overlap between significant cortical regions was assessed by the Dice coefficient.⁶⁹ In addition to the general factors, we presented associations in each of the twelve white matter tracts after FDR correction.

We considered two sets of adjustment. Model 1 included age and sex; macro-structural global measures were also corrected for the premorbid brain size by adjusting for intracranial volume. Model 2 additionally adjusted for confounders picked individually for each life-course model using a directed acyclic graph (Supplementary Figure 9). Father's social class and *APOE* $\epsilon 4$ allele status were confounders for all life-course models, childhood IQ and education for young adulthood, mid- to late adulthood and accumulation models, while adult occupational social class for mid- to late adulthood and accumulation models. Analyses for local and regional global brain measures were performed with both Model 1 and Model 2 adjustments, exploratory and sensitivity analysis were estimated using Model 2 adjustments (if applicable).

We performed exploratory analyses to test whether the associations between neighbourhood deprivation and global brain structure differed by sex, *APOE* $\epsilon 4$ allele status, father's social class, and own adult social class. Models were fitted with interaction terms; population groups with FDR-significant differences were carried forward to multi-group SEM analysis. Six sensitivity analyses tested the robustness of associations with global brain measures. First, to address high correlation between neighbourhood deprivation scores across the three epochs, we regressed young adulthood on childhood scores, mid- to late adulthood on young adulthood scores within SEM by preserving their temporal ordering (S1). Second, we adjusted all models for stroke identified from MRI scans (S2). Third, mid- to late adulthood models were further adjusted for health-related variables (i.e., BMI, smoking status, self-reported medical diagnoses) (S3). For sensitivity analysis 2 and 3, we presented % change in standardized coefficients to aid comparison with the main model (i.e., Model 2). Fourth, we applied a strict criterion for computing life-course exposures: participants were required to have valid neighbourhood deprivation scores (i.e., live in the City of Edinburgh) for each decade within a sensitive period, and for each decade during their lives for the accumulated deprivation model (S4). Fifth, to reduce bias from recall inaccuracy during residential history recollection we excluded participants with cognitive impairment⁵³, identified as either reporting dementia or scoring <24 at the Mini-Mental State Examination in any of the available LBC1936 follow-up waves (Waves 1-5) (S5). Sixth, we presented main analysis with traditionally performed linear regression with complete cases (S6).

ACKNOWLEDGEMENTS

The LBC1936 study was conducted according to the Declaration of Helsinki guidelines with ethical permission obtained from the Multi-Centre Research Ethics Committee for Scotland (MREC/01/0/56), Lothian Research Ethics Committee (Wave 1, LREC/2003/2/29), and the Scotland A Research Ethics Committee (Waves 2-4, 07/MRE00/58). Written consent was obtained from all participants.

AUTHOR CONTRIBUTIONS

IJD and SRC obtained and managed the core LBC1936 dataset, JP obtained and processed the geographic data, and SMM, MVH, EB, MB, JW, IJD and SRC conducted the MRI acquisition and image processing. GB, IJD, SRC and JP conceived and designed the study. GB performed the main statistical analyses, CRB the vertex-wise analysis. ELSC prepared the glass brain plots (i.e., Figure 2B, Supplementary Figure 8). GB led the manuscript preparations, drafting and revisions. All authors participated in the interpretation of the findings, critically revised the manuscript, and approved the final version.

FUNDING

This work was supported by the Economic and Social Research Council, UK (ESRC; grant award ES/T003669/1). The LBC1936 study is supported by the Biotechnology and Biological Sciences Research Council (BBSRC) and the ESRC (BB/W008793/1), Age UK (Disconnected Mind project), the US National Institutes of Health (R01AG054628, which supports IJD), and the University of Edinburgh. SRC was supported by a Sir Henry Dale Fellowship jointly funded by the Wellcome Trust and the Royal Society (221890/Z/20/Z); ELSC was supported by the Wellcome Trust (108890/Z/15/Z). The Lothian Birth Cohort 1936 study acknowledges the financial support of NHS Research Scotland (NRS), through Edinburgh Clinical Research

Facility. We gratefully acknowledge the contributions of the LBC1936 participants and members of the LBC1936 research team who collect and manage the LBC data.

DATA AVAILABILITY

The LBCs' study data have been the subject of many internal (within the University of Edinburgh) and external collaborations, which are encouraged. Those who have interests in outcomes other than cognitive domains are particularly encouraged to collaborate. Both LBC studies have clear data dictionaries which help researchers to discern whether the variables they wish to use are present; these provide a simple short title for each variable, alongside a longer, common-sense description/provenance of each variable. This information is available on the study website (<https://www.ed.ac.uk/lothian-birth-cohorts>) alongside comprehensive data grids listing all variables collected throughout both LBC studies and the wave at which they were introduced, an 'LBC Data Request Form' and example Data Transfer Agreement. Initially, the Data Request Form is e-mailed to the Lothian Birth Cohorts Director Dr Simon R. Cox for approval (via a panel comprising study co-investigators). Instances where approved projects require transfer of data or materials outside the University of Edinburgh require a formal Data Transfer Agreement or Material Transfer Agreement to be established with the host institution. The process is facilitated by a full-time LBC database manager – there is no charge.

For the purpose of open access, the author has applied a Creative Commons Attribution (CC BY) licence to any Author Accepted Manuscript version arising from this submission.

COMPETING INTERESTS

The authors declare no competing interests.

REFERENCES

- 1 United Nations Department of Economic and Social Affairs Population Division. World Population Ageing 2020 Highlights: Living arrangements of older persons. Report No. (ST/ESA/SER.A/451), (United Nations, New York, USA, 2020).
- 2 Nichols, E. *et al.* Estimation of the global prevalence of dementia in 2019 and forecasted prevalence in 2050: an analysis for the Global Burden of Disease Study 2019. *Lancet Public Health* **7**, e105-e125 (2022).
- 3 Röhr, S. *et al.* Estimating prevalence of subjective cognitive decline in and across international cohort studies of aging: a COSMIC study. *Alzheimer's Res Ther* **12**, 167 (2020).
- 4 Cox, S. R. & Deary, I. J. Brain and cognitive ageing: The present, and some predictions (...about the future). *Aging Brain* **2**, 100032 (2022).
- 5 Deary, I. J., Cox, S. R. & Hill, W. D. Genetic variation, brain, and intelligence differences. *Molecular Psychiatry* **27**, 335-353 (2022).
- 6 Cox, S. R., Ritchie, S. J., Fawns-Ritchie, C., Tucker-Drob, E. M. & Deary, I. J. Structural brain imaging correlates of general intelligence in UK Biobank. *Intelligence* **76**, 101376 (2019).
- 7 Baranyi, G. *et al.* Neighbourhood deprivation across eight decades and late-life cognitive function in the Lothian Birth Cohort 1936: A life-course study. *medRxiv*, (2022).
- 8 Besser, L. M., McDonald, N. C., Song, Y., Kukull, W. A. & Rodriguez, D. A. Neighborhood Environment and Cognition in Older Adults: A Systematic Review. *Am J Prev Med* **53**, 241-251 (2017).
- 9 Hunt, J. F. V. *et al.* Association of Neighborhood-Level Disadvantage With Cerebral and Hippocampal Volume. *JAMA Neurology* **77**, 451-460 (2020).

- 10 Hunt, J. F. V. *et al.* Association of Neighborhood Context, Cognitive Decline, and Cortical Change in an Unimpaired Cohort. *Neurology* **96**, e2500-e2512 (2021).
- 11 Rosso, A. L. *et al.* Neighborhood Socioeconomic Status and Cognitive Function in Late Life. *Am J Epidemiol* **183**, 1088-1097 (2016).
- 12 Gianaros, P. J. *et al.* Community Socioeconomic Disadvantage in Midlife Relates to Cortical Morphology via Neuroendocrine and Cardiometabolic Pathways. *Cereb Cortex* **27**, 460-473 (2017).
- 13 Ailshire, J., Karraker, A. & Clarke, P. Neighborhood social stressors, fine particulate matter air pollution, and cognitive function among older U.S. adults. *Soc Sci Med* **172**, 56-63 (2017).
- 14 Gianaros, P. J., Marsland, A. L., Sheu, L. K., Erickson, K. I. & Verstynen, T. D. Inflammatory pathways link socioeconomic inequalities to white matter architecture. *Cereb Cortex* **23**, 2058-2071 (2013).
- 15 Cox, S. R. *et al.* Ageing and brain white matter structure in 3,513 UK Biobank participants. *Nat Commun* **7**, 13629 (2016).
- 16 Jones, D. K., Knösche, T. R. & Turner, R. White matter integrity, fiber count, and other fallacies: the do's and don'ts of diffusion MRI. *Neuroimage* **73**, 239-254 (2013).
- 17 Salthouse, T. A. Trajectories of normal cognitive aging. *Psychol Aging* **34**, 17-24 (2019).
- 18 Amieva, H. *et al.* Prodromal Alzheimer's disease: successive emergence of the clinical symptoms. *Ann Neurol* **64**, 492-498 (2008).
- 19 Besser, L. M., Brenowitz, W. D., Meyer, O. L., Hoermann, S. & Renne, J. Methods to Address Self-Selection and Reverse Causation in Studies of Neighborhood Environments and Brain Health. *Int J Environ Res Public Health* **18**, 6484 (2021).

- 20 Gustafsson, P. E. *et al.* Residential Selection across the Life Course: Adolescent Contextual and Individual Determinants of Neighborhood Disadvantage in Mid-Adulthood. *PLOS ONE* **8**, e80241 (2013).
- 21 Kuh, D., Ben-Shlomo, Y., Lynch, J., Hallqvist, J. & Power, C. Life course epidemiology. *J Epidemiol Community Health* **57**, 778-783 (2003).
- 22 Backhouse, E. V. *et al.* Early life predictors of late life cerebral small vessel disease in four prospective cohort studies. *Brain* **144**, 3769-3778 (2021).
- 23 Pearce, J., Cherrie, M., Shortt, N., Deary, I. & Ward Thompson, C. Life course of place: A longitudinal study of mental health and place. *Trans Inst Br Geogr* **43**, 555-572 (2018).
- 24 Hedman, A. M., van Haren, N. E., Schnack, H. G., Kahn, R. S. & Hulshoff Pol, H. E. Human brain changes across the life span: a review of 56 longitudinal magnetic resonance imaging studies. *Hum Brain Mapp* **33**, 1987-2002 (2012).
- 25 Bethlehem, R. A. I. *et al.* Brain charts for the human lifespan. *Nature* **604**, 525-533 (2022).
- 26 Krishnadas, R. *et al.* Socioeconomic deprivation and cortical morphology: psychological, social, and biological determinants of ill health study. *Psychosom Med* **75**, 616-623 (2013).
- 27 Fan, L. *et al.* The Human Brainnetome Atlas: A New Brain Atlas Based on Connectional Architecture. *Cerebral Cortex* **26**, 3508-3526 (2016).
- 28 Besser, L. M. *et al.* Associations between neighborhood greenspace and brain imaging measures in non-demented older adults: the Cardiovascular Health Study. *Soc Psychiatry Psychiatr Epidemiol* **56**, 1575-1585 (2021).

- 29 Rakesh, D., Zalesky, A. & Whittle, S. Assessment of Parent Income and Education, Neighborhood Disadvantage, and Child Brain Structure. *JAMA Netw Open* **5**, e2226208 (2022).
- 30 Parker, N. *et al.* Income inequality, gene expression, and brain maturation during adolescence. *Sci Rep* **7**, 7397 (2017).
- 31 Johnson, S. B., Riis, J. L. & Noble, K. G. State of the Art Review: Poverty and the Developing Brain. *Pediatrics* **137** (2016).
- 32 Mackes, N. K. *et al.* Early childhood deprivation is associated with alterations in adult brain structure despite subsequent environmental enrichment. *Proceedings of the National Academy of Sciences* **117**, 641-649 (2020).
- 33 Hackman, D. A. *et al.* Association of Local Variation in Neighborhood Disadvantage in Metropolitan Areas With Youth Neurocognition and Brain Structure. *JAMA Pediatr* **175**, e210426 (2021).
- 34 Taylor, R. L., Cooper, S. R., Jackson, J. J. & Barch, D. M. Assessment of Neighborhood Poverty, Cognitive Function, and Prefrontal and Hippocampal Volumes in Children. *JAMA Network Open* **3**, e2023774-e2023774 (2020).
- 35 Lean, R. E. *et al.* Prenatal exposure to maternal social disadvantage and psychosocial stress and neonatal white matter connectivity at birth. *Proc Natl Acad Sci U S A* **119**, e2204135119 (2022).
- 36 Triplett, R. L. *et al.* Association of Prenatal Exposure to Early-Life Adversity With Neonatal Brain Volumes at Birth. *JAMA Network Open* **5**, e227045-e227045 (2022).
- 37 Johnson, A., Bathelt, J., Akarca, D., Crickmore, G. & Astle, D. E. Far and wide: Associations between childhood socio-economic status and brain connectomics. *Dev Cogn Neurosci* **48**, 100888 (2021).

- 38 Bell, K. L. *et al.* White Matter Microstructure in the Young Adult Brain Varies with Neighborhood Disadvantage in Adolescence. *Neuroscience* **466**, 162-172 (2021).
- 39 Gard, A. M. *et al.* Beyond family-level adversities: Exploring the developmental timing of neighborhood disadvantage effects on the brain. *Dev Sci* **24**, e12985 (2021).
- 40 Whalley, L. J., Deary, I. J., Appleton, C. L. & Starr, J. M. Cognitive reserve and the neurobiology of cognitive aging. *Ageing Research Reviews* **3**, 369-382 (2004).
- 41 Prior, L. Allostatic Load and Exposure Histories of Disadvantage. *Int J Environ Res Public Health* **18**, 7222 (2021).
- 42 Bentley, R. & Baker, E. Placing a housing lens on neighbourhood disadvantage, socioeconomic position and mortality. *Lancet Public Health* **7**, e396-e397 (2022).
- 43 Sampson, R. J., Raudenbush, S. W. & Earls, F. Neighborhoods and violent crime: a multilevel study of collective efficacy. *Science* **277**, 918-924 (1997).
- 44 Astell-Burt, T., Feng, X., Mavoa, S., Badland, H. M. & Giles-Corti, B. Do low-income neighbourhoods have the least green space? A cross-sectional study of Australia's most populous cities. *BMC Public Health* **14**, 292 (2014).
- 45 Brazil, N. Environmental inequality in the neighborhood networks of urban mobility in US cities. *Proc Natl Acad Sci U S A* **119**, e2117776119 (2022).
- 46 Macdonald, L., Olsen, J. R., Shortt, N. K. & Ellaway, A. Do 'environmental bads' such as alcohol, fast food, tobacco, and gambling outlets cluster and co-locate in more deprived areas in Glasgow City, Scotland? *Health Place* **51**, 224-231 (2018).
- 47 Power, M. C. *et al.* The Association of Long-Term Exposure to Particulate Matter Air Pollution with Brain MRI Findings: The ARIC Study. *Environ Health Perspect* **126** (2018).

- 48 Johnson, W., Corley, J., Starr, J. M. & Deary, I. J. Psychological and physical health at age 70 in the Lothian Birth Cohort 1936: links with early life IQ, SES, and current cognitive function and neighborhood environment. *Health Psychol* **30**, 1-11 (2011).
- 49 Calvin, C. M. *et al.* Childhood intelligence in relation to major causes of death in 68 year follow-up: prospective population study. *BMJ* **357**, j2708 (2017).
- 50 Taylor, A. M., Pattie, A. & Deary, I. J. Cohort Profile Update: The Lothian Birth Cohorts of 1921 and 1936. *Int J Epidemiol* **47**, 1042-1042r (2018).
- 51 Deary, I. J. *et al.* The Lothian Birth Cohort 1936: a study to examine influences on cognitive ageing from age 11 to age 70 and beyond. *BMC geriatrics* **7**, 28-28 (2007).
- 52 Morgan, O. & Baker, A. Measuring deprivation in England and Wales using 2001 Carstairs scores. *Health Stat Q* **31**, 28-33 (2006).
- 53 Baranyi, G. *et al.* Association of Life-Course Neighborhood Deprivation With Frailty and Frailty Progression From Ages 70 to 82 Years in the Lothian Birth Cohort 1936. *American Journal of Epidemiology* **191**, 1856-1866 (2022).
- 54 Wardlaw, J. M. *et al.* Brain Ageing, Cognition in Youth and Old Age, and Vascular Disease in the Lothian Birth Cohort 1936: Rationale, Design and Methodology of the Imaging Protocol. *International Journal of Stroke* **6**, 547-559 (2011).
- 55 Clayden, J. D. *et al.* TractoR: Magnetic Resonance Imaging and Tractography with R. *Journal of Statistical Software* **44**, 1 – 18 (2011).
- 56 Smith, S. M. *et al.* Advances in functional and structural MR image analysis and implementation as FSL. *NeuroImage* **23**, S208-S219 (2004).
- 57 Smith, S. M. Fast robust automated brain extraction. *Human Brain Mapping* **17**, 143-155 (2002).
- 58 Jenkinson, M. & Smith, S. A global optimisation method for robust affine registration of brain images. *Med Image Anal* **5**, 143-156 (2001).

- 59 Behrens, T. E. J., Berg, H. J., Jbabdi, S., Rushworth, M. F. S. & Woolrich, M. W. Probabilistic diffusion tractography with multiple fibre orientations: What can we gain? *NeuroImage* **34**, 144-155 (2007).
- 60 Behrens, T. E. J. *et al.* Characterization and propagation of uncertainty in diffusion-weighted MR imaging. *Magn Reson Med* **50**, 1077-1088 (2003).
- 61 Conole, E. L. S. *et al.* DNA Methylation and Protein Markers of Chronic Inflammation and Their Associations With Brain and Cognitive Aging. *Neurology* **97**, e2340-e2352 (2021).
- 62 Corley, J. *et al.* Predictors of longitudinal cognitive ageing from age 70 to 82 including APOE e4 status, early-life and lifestyle factors: the Lothian Birth Cohort 1936. *Mol Psychiatry* **28**, 1256-1271 (2022).
- 63 Office of Population Censuses and Surveys. Classification of Occupations and Coding Index. (HMSO, London, UK, 1980).
- 64 Rosseel, Y. lavaan: An R Package for Structural Equation Modeling. *J Stat Softw* **48**, 1-36 (2012).
- 65 R: A language and environment for statistical computing (R Foundation for Statistical Computing, Vienna, Austria, 2022).
- 66 Lee, T. & Shi, D. A comparison of full information maximum likelihood and multiple imputation in structural equation modeling with missing data. *Psychol Methods* **26**, 466-485 (2021).
- 67 Wheater, E. *et al.* Birth weight is associated with brain tissue volumes seven decades later but not with MRI markers of brain ageing. *NeuroImage: Clinical* **31**, 102776 (2021).

- 68 Benjamini, Y. & Hochberg, Y. Controlling the False Discovery Rate: A Practical and Powerful Approach to Multiple Testing. *J R Stat Soc Ser B Methodol* **57**, 289-300 (1995).
- 69 Crum, W. R., Camara, O. & Hill, D. L. G. Generalized Overlap Measures for Evaluation and Validation in Medical Image Analysis. *IEEE Trans Med Imaging* **25**, 1451-1461 (2006).

Supplementary Material

Supplementary Table 1: Pearson's correlation coefficients between neighbourhood deprivation scores and global brain outcomes.

Supplementary Table 2: Relation of main covariates to neighbourhood deprivation scores.

Supplementary Table 3: Number of complete cases for each neighbourhood deprivation exposure and global brain measure pairs.

Supplementary Table 4: Model fit indices for general fractional anisotropy and general mean diffusivity in the main models.

Supplementary Figure 1: Regional associations between life-course models of neighbourhood deprivation and cortical volume in Model 1.

Supplementary Figure 2: Regional associations between life-course models of neighbourhood deprivation and cortical surface area in Model 1.

Supplementary Figure 3: Regional associations between life-course models of neighbourhood deprivation and cortical thickness in Model 1.

Supplementary Figure 4: Regional associations between life-course models of neighbourhood deprivation and cortical volume in Model 2.

Supplementary Figure 5: Regional associations between life-course models of neighbourhood deprivation and cortical surface area in Model 2.

Supplementary Figure 6: Regional associations between life-course models of neighbourhood deprivation and cortical thickness in Model 2.

Supplementary Figure 7: Glass brain plot locating individual white matter tracts used in the analyses.

Supplementary Table 5: Association between life-course models of neighbourhood social deprivation, fractional anisotropy, and mean diffusivity in 12 white matter tracts in Model 1.

Supplementary Table 6: Association between life-course models of neighbourhood social deprivation, fractional anisotropy, and mean diffusivity in 12 white matter tracts in Model 2.

Supplementary Table 7: Interaction of neighbourhood deprivation scores with sex, *APOE* ϵ 4 allele status and adult occupational social class and global brain outcomes.

Supplementary Table 8: Association between life-course models of neighbourhood deprivation and global brain outcomes stratified by adult social class.

Supplementary Table 9: Association between life-course models of neighbourhood deprivation and global brain outcomes after considering exposure during previous epoch.

Supplementary Table 10: Association between life-course models of neighbourhood deprivation and global brain outcomes after adjusting for stroke identified from MRI scans.

Supplementary Table 11: Association between mid-to-late adulthood neighbourhood deprivation and global brain outcomes after adjusting for late adulthood health status.

Supplementary Table 12: Association between life-course models of neighbourhood deprivation and global brain outcomes among those living in Edinburgh throughout each decade of the exposure periods.

Supplementary Table 13: Association between life-course models of neighbourhood deprivation and global brain outcomes among individuals without cognitive impairment.

Supplementary Table 14: Complete case analysis testing the association between life-course models of neighbourhood deprivation and global brain outcomes.

Supplementary Figure 8: Pearson's correlation coefficients between individual exposure to neighbourhood deprivation across decades.

Supplementary Figure 9: Directed acyclic graph representing associations between neighbourhood deprivation, global brain outcomes and confounders considered in the main and sensitivity analyses.

Supplementary Table 15: Standardized tract loadings, explained variance and goodness of fit indices for fractional anisotropy and mean diffusivity.

Supplementary Table 1: Pearson's correlation coefficients between neighbourhood deprivation scores and global brain outcomes

	Total brain volume	Grey matter volume	Normal-appearing white matter volume	White matter hyperintensity volume	Cortical surface area	Mean cortical thickness	General fractional anisotropy	General mean diffusivity	Childhood ND	Young adulthood ND	Mid- to late adulthood ND
Total brain volume											
Grey matter volume	0.92***										
Normal-appearing white matter volume	0.89***	0.75***									
White matter hyperintensity volume	0.06	-0.09*	-0.25***								
Cortical surface area	0.90***	0.80***	0.83***	0.09*							
Mean cortical thickness	0.01	0.21***	-0.10*	-0.14***	-0.16***						
General fractional anisotropy	0.15***	0.20***	0.21***	-0.34***	0.12**	0.27***					
General mean diffusivity	-0.05	-0.09*	-0.19***	0.44***	0.01	-0.12**	-0.53***				
Childhood ND	-0.07	-0.07	-0.04	-0.02	-0.08	-0.06	-0.06	0.00			
Young adulthood ND	-0.03	-0.05	0.01	-0.03	-0.07	-0.15**	-0.14**	-0.04	0.57***		
Mid- to late adulthood ND	-0.15**	-0.17***	-0.15**	0.09	-0.13*	-0.18***	-0.18***	-0.01	0.26***	0.46***	
Accumulated ND	-0.11	-0.12	-0.07	-0.03	-0.12*	-0.16	-0.10	-0.06	0.81***	0.84***	0.69***

Pairwise deletion was applied for missing values to preserve the maximum amount of available information. ND = neighbourhood deprivation.

*** $p < 0.001$

** $p < 0.01$

* $p < 0.05$

Supplementary Table 2: Relation of main covariates to neighbourhood deprivation scores

	Childhood ND		Young adulthood ND		Mid- to late adulthood ND		Accumulated ND	
	Mean (SD)	<i>p</i>	Mean (SD)	<i>p</i>	Mean (SD)	<i>p</i>	Mean (SD)	<i>p</i>
Sex								
Male	0.69 (3.51)		-0.84 (2.90)		-2.50 (2.81)		-2.01 (7.19)	
Female	0.44 (3.27)		-0.87 (2.69)		-2.19 (2.65)		-1.99 (6.47)	
Father's occupational social class								
High (professional-managerial)	-0.80 (3.38)	***	-1.79 (2.72)	***	-3.28 (2.40)	***	-5.44 (6.15)	***
Low (skilled, partly skilled and unskilled)	1.06 (3.32)		-0.54 (2.74)		-2.06 (2.76)		-0.93 (6.68)	
<i>APOE</i> ε4 allele status								
ε4 carriers	1.32 (3.25)	*	-0.56 (2.88)		-2.15 (2.90)		0.01 (6.44)	***
Not ε4 carriers	0.23 (3.39)		-1.03 (2.74)		-2.50 (2.61)		-2.96 (6.76)	
Adult occupational social class								
High (professional-managerial)	-0.13 (3.29)	***	-1.32 (2.66)	***	-2.90 (2.56)	***	-3.98 (6.08)	***
Low (skilled, partly skilled and unskilled)	1.48 (3.33)		-0.15 (2.87)		-1.47 (2.79)		0.38 (6.97)	
	Pearson's <i>r</i>	<i>p</i>	Pearson's <i>r</i>	<i>p</i>	Pearson's <i>r</i>	<i>p</i>	Pearson's <i>r</i>	<i>p</i>
Childhood IQ	-0.18	**	-0.20	***	-0.23	***	-0.25	***
Years spent in education	-0.27	***	-0.28	***	-0.36	***	-0.42	***

Pairwise deletion was applied for missing values to preserve the maximum amount of available information. Statistical analyses were based on two-sample t-tests for mean differences, and Pearson's correlation for associations between continuous variables. ND = neighbourhood deprivation.

*** $p < 0.001$

** $p < 0.01$

* $p < 0.05$

Supplementary Table 3: Number of complete cases for each neighbourhood deprivation exposure and global brain measure pairs.

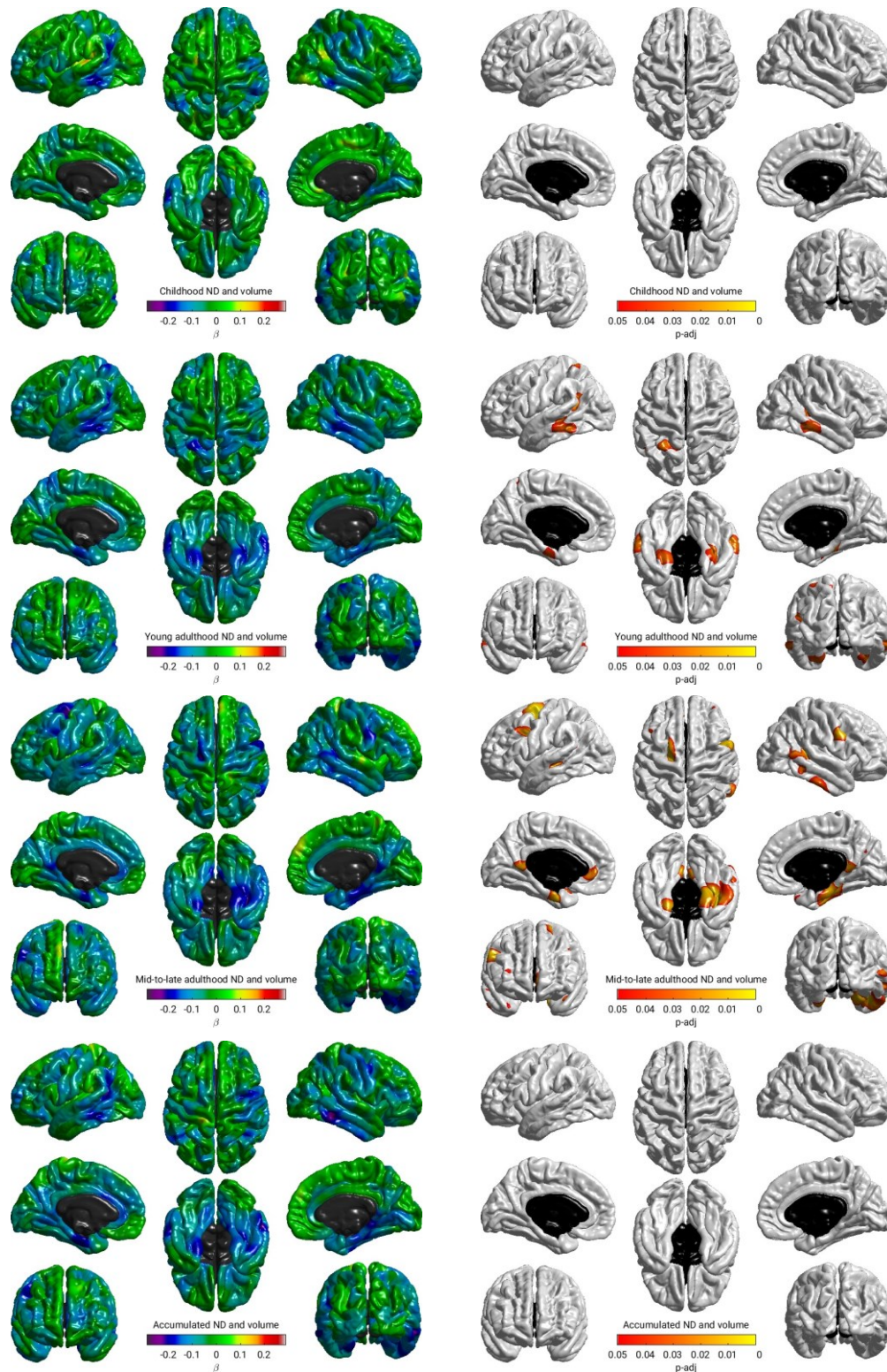
	Childhood	Young adulthood	Mid- to late adulthood	Accumulated
Total brain volume ($N=658$)	$n=305$	$n=376$	$n=390$	$n=276$
Grey matter volume ($N=658$)	$n=305$	$n=376$	$n=390$	$n=276$
Normal-appearing white matter volume ($N=658$)	$n=305$	$n=376$	$n=390$	$n=276$
White matter hyperintensity volume ($N=672$)	$n=311$	$n=383$	$n=396$	$n=281$
Cortical surface area ($N=636$)	$n=296$	$n=367$	$n=379$	$n=268$
Mean cortical thickness ($N=636$)	$n=296$	$n=367$	$n=379$	$n=268$
General fractional anisotropy ($N=665$)	$n=307$	$n=376$	$n=388$	$n=276$
General mean diffusivity ($N=665$)	$n=307$	$n=376$	$n=388$	$n=276$

Supplementary Table 4: Model fit indices for general fractional anisotropy and general mean diffusivity in the main models

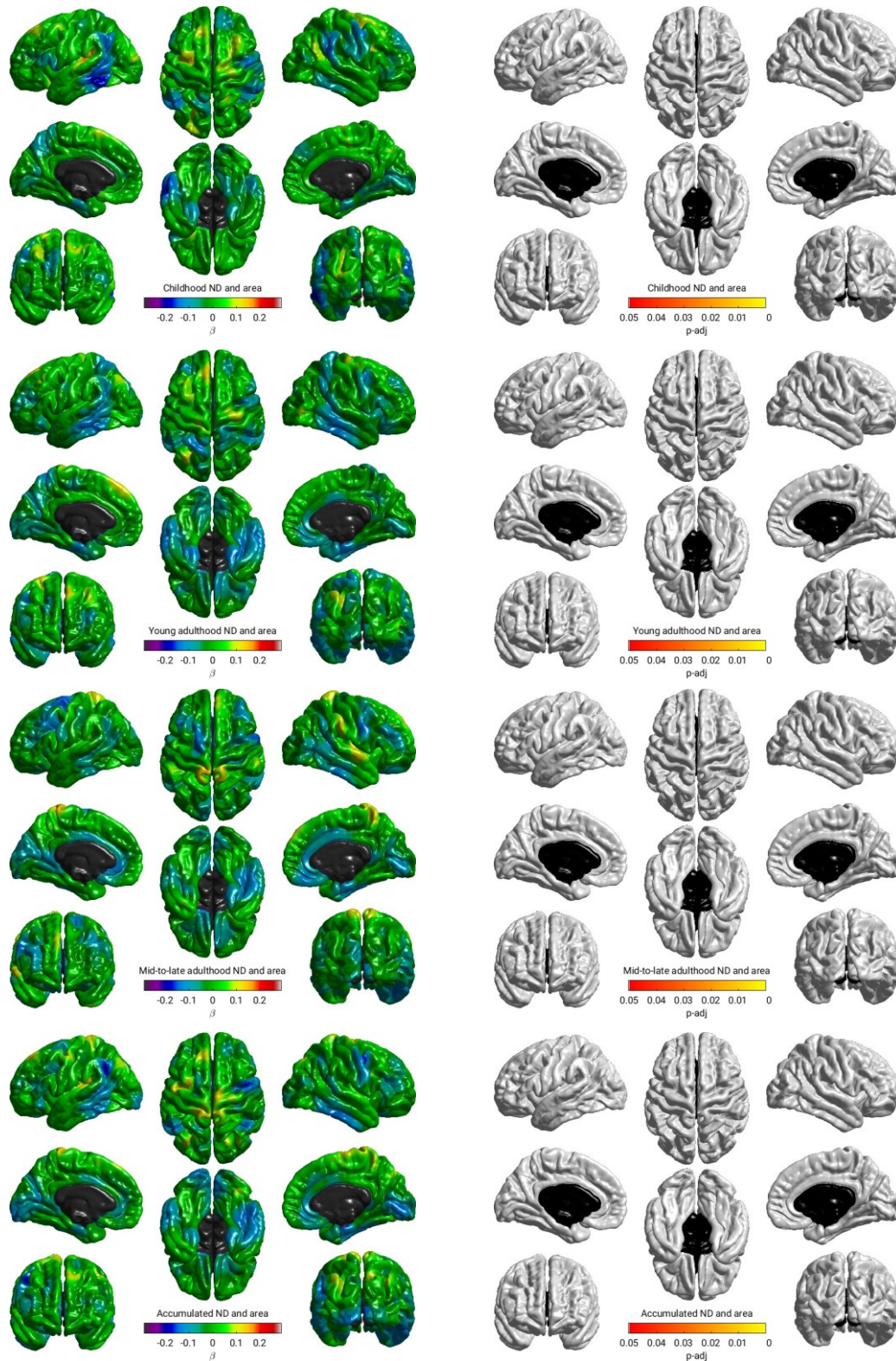
	Model 1				Model 2			
	CFI	TLI	RMSEA	SRMR	CFI	TLI	RMSEA	SRMR
<i>Childhood neighbourhood deprivation</i>								
General fractional anisotropy	0.95	0.93	0.05	0.04	0.93	0.91	0.06	0.04
General mean diffusivity	0.95	0.94	0.04	0.04	0.93	0.92	0.05	0.04
<i>Young adulthood neighbourhood deprivation</i>								
General fractional anisotropy	0.95	0.93	0.05	0.04	0.94	0.93	0.04	0.04
General mean diffusivity	0.93	0.91	0.06	0.04	0.93	0.91	0.05	0.04
<i>Mid- to late adulthood neighbourhood deprivation</i>								
General fractional anisotropy	0.94	0.92	0.05	0.04	0.94	0.93	0.04	0.04
General mean diffusivity	0.93	0.91	0.06	0.05	0.92	0.91	0.05	0.04
<i>Accumulated neighbourhood deprivation</i>								
General fractional anisotropy	0.94	0.93	0.05	0.04	0.94	0.93	0.04	0.04
General mean diffusivity	0.93	0.91	0.06	0.04	0.93	0.91	0.05	0.04

Reference values are: CFI>0.95, TLI>0.95, RMSEA<0.06, SRMR<0.08 (1). CFI=Comparative Fit Index; TLI= Tucker-Lewis Index; RMSEA=Root Mean Square Error of Approximation; SRMR=Standardized Root Mean Square Residual

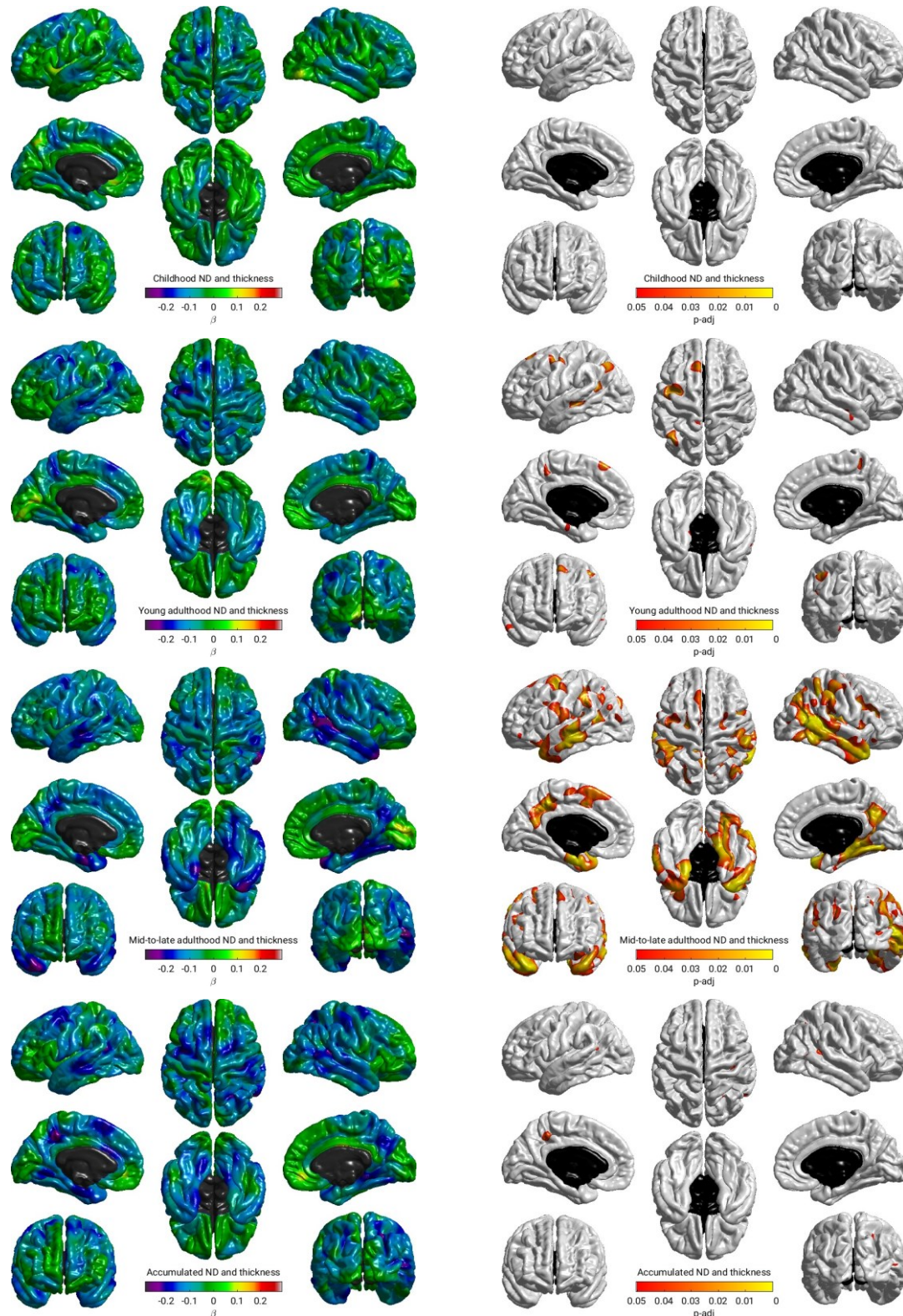
Supplementary Figure 1: Regional associations between life-course models of neighbourhood deprivation and cortical volume in Model 1. Standardized coefficients were obtained in linear regression models fitted within the structural equation modelling framework applying full information maximum likelihood estimation. Sample size was $N=622$; pairwise complete observations were $n=289$, $n=358$, $n=371$ and $n=262$ for childhood, young adulthood, mid-to-late adulthood, and accumulated neighbourhood deprivation (ND), respectively. Models were adjusted for sex, age, and intracranial volume. Heatmaps show (from left to right): standardised betas and false discovery rate adjusted p -values ($p_{FDR} < 0.05$). The non-cortical mask is shown in black.



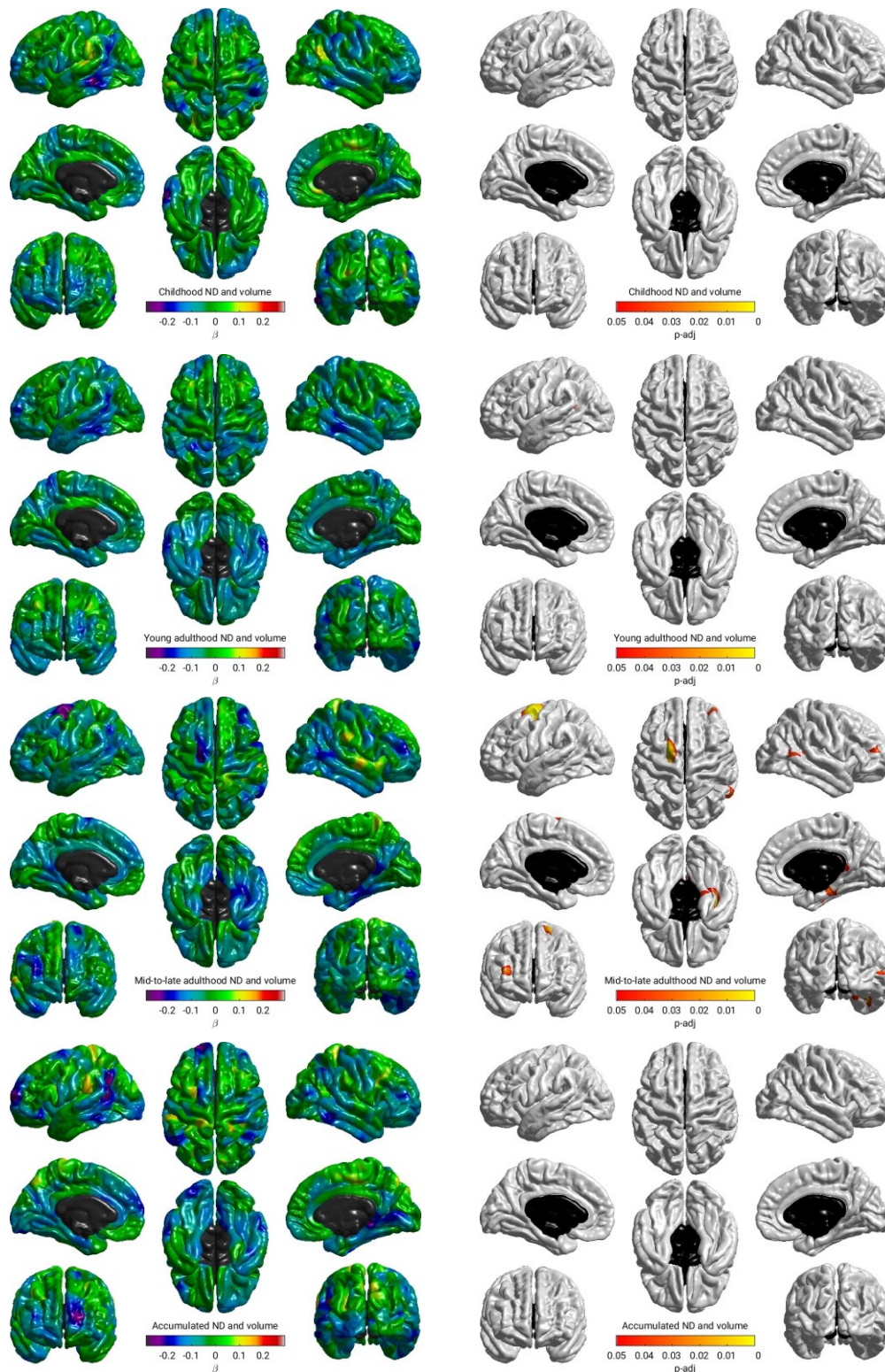
Supplementary Figure 2: Regional associations between life-course models of neighbourhood deprivation and cortical surface area in Model 1. Standardized coefficients were obtained in linear regression models fitted within the structural equation modelling framework applying full information maximum likelihood estimation. Sample size was $N=622$; pairwise complete observations were $n=289$, $n=358$, $n=371$ and $n=262$ for childhood, young adulthood, mid-to-late adulthood, and accumulated neighbourhood deprivation (ND), respectively. Models were adjusted for sex, age, and intracranial volume. Heatmaps show (from left to right): standardised betas and false discovery rate adjusted p -values ($p_{FDR} < 0.05$). The non-cortical mask is shown in black.



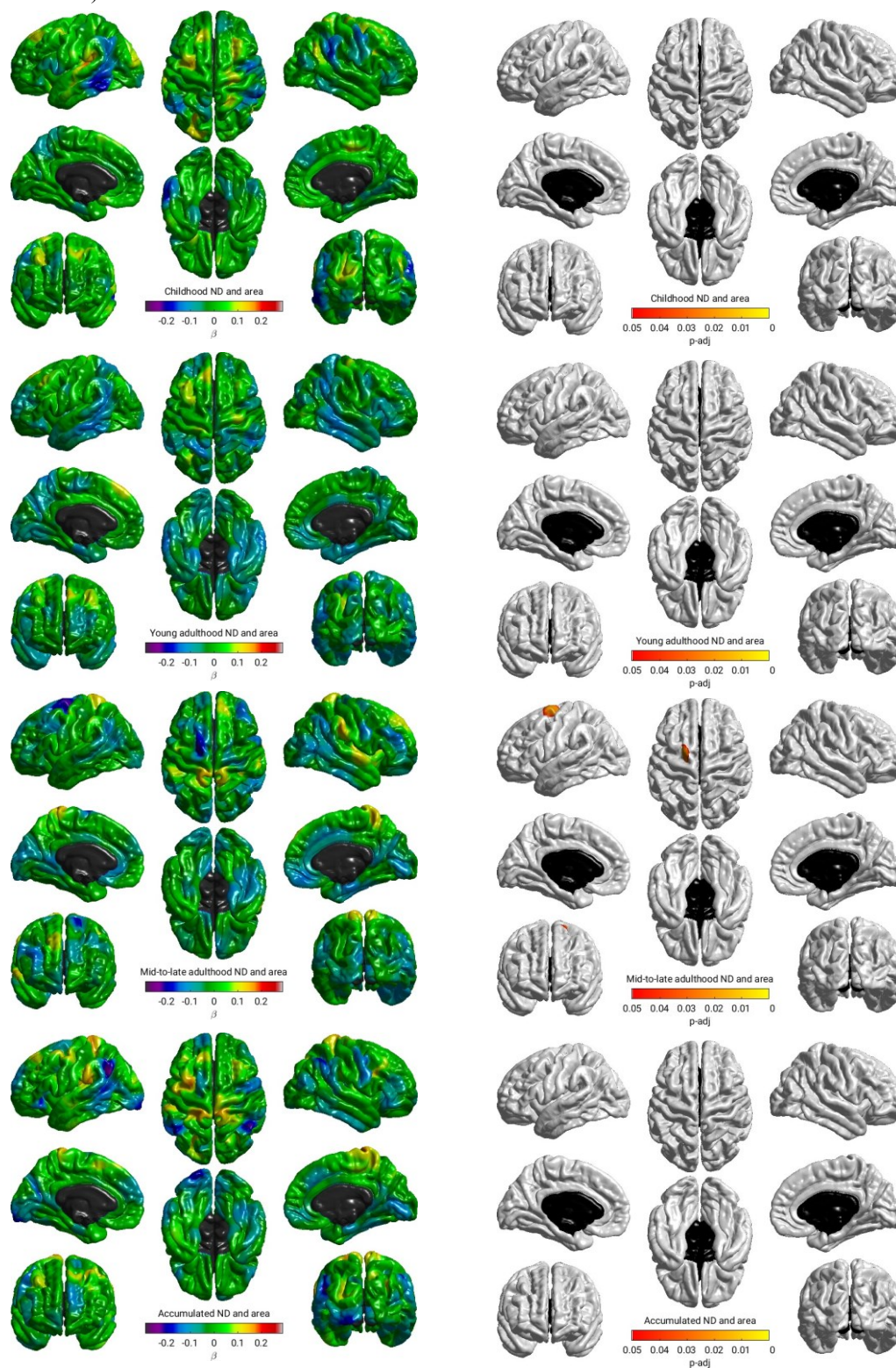
Supplementary Figure 3: Regional associations between life-course models of neighbourhood deprivation and cortical thickness in Model 1. Standardized coefficients were obtained in linear regression models fitted within the structural equation modelling framework applying full information maximum likelihood estimation. Sample size was $N=622$; pairwise complete observations were $n=289$, $n=358$, $n=371$ and $n=262$ for childhood, young adulthood, mid-to-late adulthood, and accumulated neighbourhood deprivation (ND), respectively. Models were adjusted for sex, age, and intracranial volume. Heatmaps show (from left to right): standardised betas and false discovery rate adjusted p -values ($p_{FDR} < 0.05$). The non-cortical mask is shown in black.



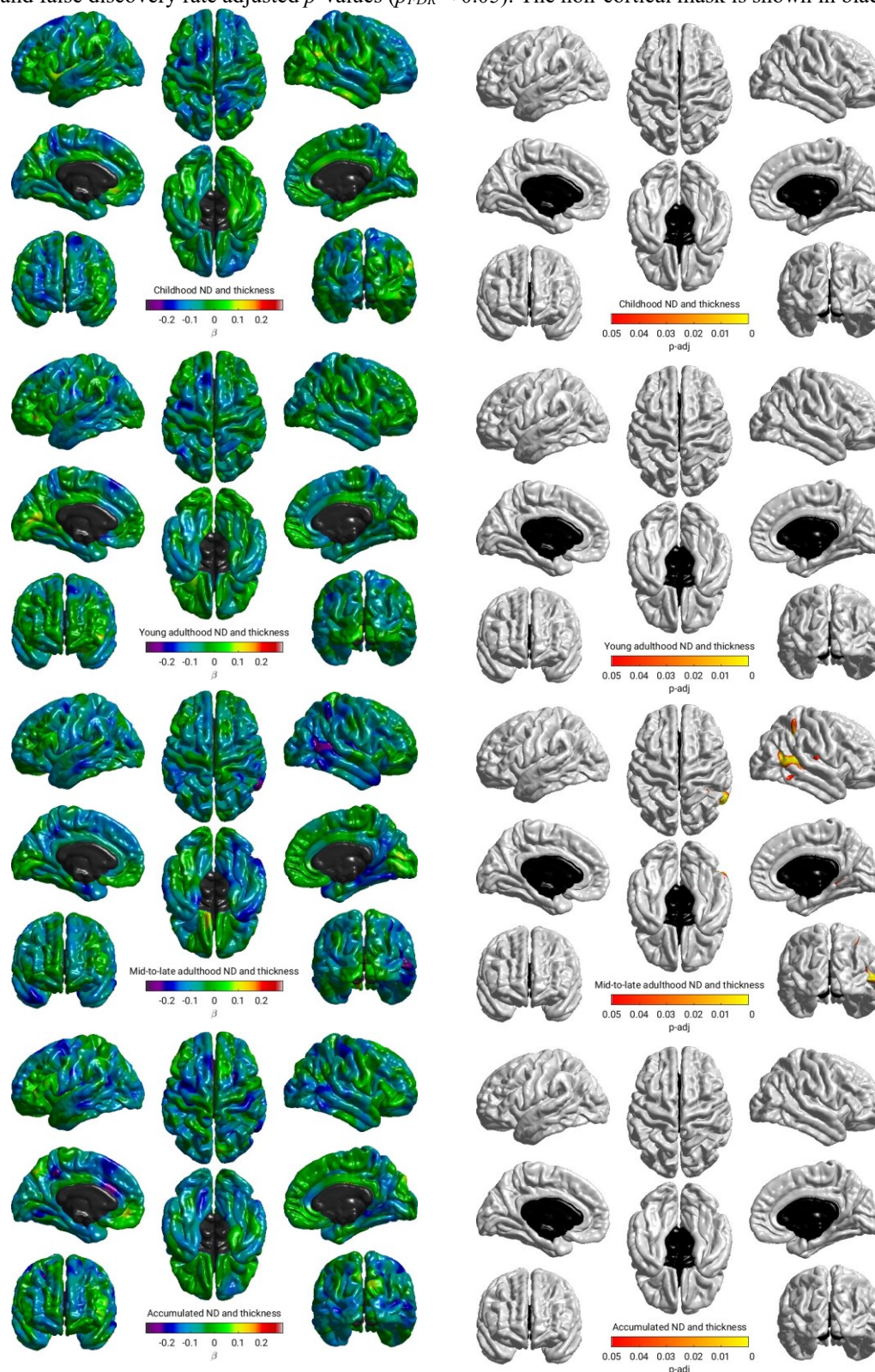
Supplementary Figure 4: Regional associations between life-course models of neighbourhood deprivation and cortical volume in Model 2. Standardized coefficients were obtained in linear regression models fitted within the structural equation modelling framework applying full information maximum likelihood estimation. Sample size was $N=622$; pairwise complete observations were $n=289$, $n=358$, $n=371$ and $n=262$ for childhood, young adulthood, mid-to-late adulthood, and accumulated neighbourhood deprivation (ND), respectively. Models were adjusted for sex, age, intracranial volume, father's occupational social class, APOE $\epsilon 4$ allele status. In addition, young adulthood models were adjusted for childhood IQ and years spent in education, and mid- to late adulthood/ accumulation models also for adult occupational social class. Heatmaps show (from left to right): standardised betas and false discovery rate adjusted p -values ($p_{FDR} < 0.05$). The non-cortical mask is shown in black.



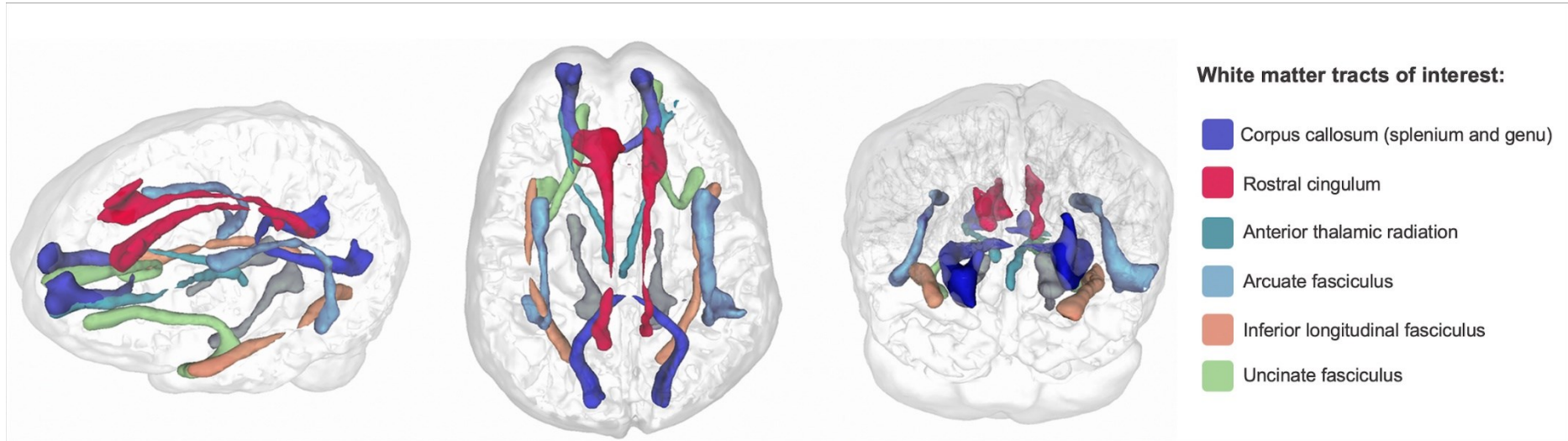
Supplementary Figure 5: Regional associations between life-course models of neighbourhood deprivation and cortical surface area in Model 2. Standardized coefficients were obtained in linear regression models fitted within the structural equation modelling framework applying full information maximum likelihood estimation. Sample size was $N=622$; pairwise complete observations were $n=289$, $n=358$, $n=371$ and $n=262$ for childhood, young adulthood, mid-to-late adulthood, and accumulated neighbourhood deprivation (ND), respectively. Models were adjusted for sex, age, intracranial volume, father's occupational social class, APOE $\epsilon 4$ allele status. In addition, young adulthood models were adjusted for childhood IQ and years spent in education, and mid- to late adulthood/ accumulation models also for adult occupational social class. Heatmaps show (from left to right): standardised betas and false discovery rate adjusted p -values ($p_{FDR} < 0.05$). The non-cortical mask is shown in black.



Supplementary Figure 6: Regional associations between life-course models of neighbourhood deprivation and cortical thickness in Model 2. Standardized coefficients were obtained in linear regression models fitted within the structural equation modelling framework applying full information maximum likelihood estimation. Sample size was $N=622$; pairwise complete observations were $n=289$, $n=358$, $n=371$ and $n=262$ for childhood, young adulthood, mid-to-late adulthood, and accumulated neighbourhood deprivation (ND), respectively. Models were adjusted for sex, age, intracranial volume, father's occupational social class, APOE $\epsilon 4$ allele status. In addition, young adulthood models were adjusted for childhood IQ and years spent in education, and mid- to late adulthood/accumulation models also for adult occupational social class. Heatmaps show (from left to right): standardised betas and false discovery rate adjusted p -values ($p_{FDR} < 0.05$). The non-cortical mask is shown in black.



Supplementary Figure 7: Glass brain plot locating white matter tracts used in the analyses. The ventral cingulum, coloured in grey, was not included in analyses as the rostral and ventral cingula are subdivisions of the same tract (an approach adopted previously in this cohort, e.g., (2))



Supplementary Table 5: Association between life-course models of neighbourhood deprivation, fractional anisotropy and mean diffusivity in 12 white matter tracts in Model 1

	Fractional anisotropy				Mean diffusivity			
	β	SE	p	p_{FDR}	β	SE	p	p_{FDR}
<i>Childhood neighbourhood deprivation (n=279 to 306)</i>								
Genu of corpus callosum	0.04	0.06	0.54	0.82	-0.02	0.06	0.72	0.95
Splenium of corpus callosum	-0.06	0.06	0.28	0.82	0.06	0.06	0.31	0.95
Left arcuate fasciculus	-0.03	0.05	0.61	0.82	0.00	0.06	0.99	0.99
Right arcuate fasciculus	-0.04	0.06	0.47	0.82	0.03	0.06	0.59	0.95
Left anterior thalamic radiation	-0.07	0.06	0.22	0.82	0.00	0.06	0.98	0.99
Right anterior thalamic radiation	0.00	0.06	0.97	0.97	-0.09	0.06	0.13	0.90
Left rostral cingulum	-0.09	0.06	0.13	0.82	0.03	0.06	0.64	0.95
Right rostral cingulum	-0.01	0.05	0.86	0.94	-0.03	0.06	0.61	0.95
Left inferior longitudinal fasciculus	0.02	0.06	0.68	0.82	-0.04	0.07	0.56	0.95
Right inferior longitudinal fasciculus	0.03	0.05	0.56	0.82	-0.08	0.06	0.15	0.90
Left uncinate fasciculus	-0.07	0.06	0.27	0.82	0.03	0.06	0.59	0.95
Right uncinate fasciculus	-0.03	0.06	0.63	0.82	0.02	0.06	0.79	0.95
<i>Young adulthood neighbourhood deprivation (n=346 to 375)</i>								
Genu of corpus callosum	-0.01	0.05	0.80	0.87	-0.08	0.05	0.15	0.58
Splenium of corpus callosum	0.00	0.05	0.95	0.95	-0.02	0.05	0.70	0.79
Left arcuate fasciculus	-0.09	0.05	0.06	0.25	-0.06	0.05	0.26	0.64
Right arcuate fasciculus	-0.03	0.05	0.51	0.62	-0.01	0.06	0.80	0.80
Left anterior thalamic radiation	-0.03	0.05	0.52	0.62	-0.10	0.05	0.05	0.58
Right anterior thalamic radiation	-0.05	0.05	0.30	0.51	-0.08	0.05	0.15	0.58
Left rostral cingulum	-0.07	0.05	0.21	0.51	-0.03	0.05	0.57	0.79
Right rostral cingulum	-0.04	0.05	0.40	0.59	-0.06	0.05	0.27	0.64
Left inferior longitudinal fasciculus	-0.06	0.05	0.30	0.51	0.06	0.06	0.37	0.73
Right inferior longitudinal fasciculus	-0.09	0.05	0.06	0.25	0.02	0.06	0.69	0.79
Left uncinate fasciculus	-0.11	0.05	0.04	0.25	-0.02	0.05	0.72	0.79
Right uncinate fasciculus	-0.09	0.05	0.08	0.25	0.02	0.06	0.73	0.79
<i>Mid- to late adulthood neighbourhood deprivation (n=359 to 387)</i>								
Genu of corpus callosum	0.02	0.05	0.68	0.74	-0.08	0.05	0.13	0.39
Splenium of corpus callosum	-0.14	0.05	0.01	0.03	0.08	0.06	0.16	0.39
Left arcuate fasciculus	-0.13	0.05	0.01	0.03	0.03	0.05	0.55	0.70
Right arcuate fasciculus	-0.11	0.05	0.05	0.12	0.00	0.06	0.97	0.97
Left anterior thalamic radiation	-0.08	0.05	0.12	0.17	-0.08	0.05	0.12	0.39
Right anterior thalamic radiation	-0.17	0.05	0.001	0.01	0.09	0.05	0.11	0.39
Left rostral cingulum	-0.08	0.05	0.11	0.17	-0.01	0.05	0.90	0.97
Right rostral cingulum	-0.01	0.05	0.88	0.88	-0.03	0.05	0.57	0.70
Left inferior longitudinal fasciculus	-0.08	0.05	0.11	0.17	0.05	0.06	0.38	0.70
Right inferior longitudinal fasciculus	-0.13	0.05	0.01	0.03	0.03	0.06	0.59	0.70
Left uncinate fasciculus	-0.08	0.05	0.13	0.17	-0.08	0.05	0.16	0.39
Right uncinate fasciculus	-0.05	0.05	0.38	0.46	-0.04	0.06	0.45	0.70
<i>Accumulated neighbourhood deprivation (n=251 to 275)</i>								
Genu of corpus callosum	0.04	0.06	0.54	0.66	-0.08	0.06	0.22	0.69
Splenium of corpus callosum	-0.09	0.06	0.11	0.37	0.05	0.06	0.41	0.69
Left arcuate fasciculus	-0.04	0.06	0.51	0.66	-0.07	0.06	0.25	0.69
Right arcuate fasciculus	-0.04	0.06	0.55	0.66	-0.02	0.07	0.78	0.85
Left anterior thalamic radiation	-0.04	0.06	0.51	0.66	-0.09	0.06	0.14	0.69
Right anterior thalamic radiation	-0.09	0.06	0.12	0.37	-0.05	0.06	0.39	0.69
Left rostral cingulum	-0.12	0.06	0.06	0.37	0.01	0.06	0.93	0.93
Right rostral cingulum	0.02	0.06	0.7	0.77	-0.08	0.06	0.18	0.69
Left inferior longitudinal fasciculus	-0.07	0.06	0.28	0.6	0.05	0.07	0.51	0.69
Right inferior longitudinal fasciculus	-0.09	0.06	0.1	0.37	-0.04	0.06	0.46	0.69
Left uncinate fasciculus	-0.07	0.06	0.3	0.6	-0.03	0.07	0.65	0.78
Right uncinate fasciculus	-0.01	0.06	0.84	0.84	-0.05	0.07	0.46	0.69

Models were fitted within the structural equation modelling framework applying full information maximum likelihood estimation. Total sample size was $N=633$ for genu of corpus callosum, $N=652$ for splenium of corpus callosum, $N=655$ left arcuate fasciculus, and $N=621$ for right arcuate fasciculus, $N=643$ for left anterior thalamic radiation, $N=662$ right

anterior thalamic radiation, $N=647$ for left rostral cingulum, $N=643$ for right rostral cingulum, $N=663$ for left inferior longitudinal fasciculus, $N=663$ for left and right inferior longitudinal fasciculus, $N=618$ for left uncinate fasciculus and $N=647$ for right uncinate fasciculus; this table indicates ranges of observations for each exposure-outcomes pairs on which reported effect sizes are based (n). Bold typeface denotes false discovery rate adjusted significance (p_{FDR}). SE = standard error.

All models were adjusted for sex and age.

Supplementary Table 6: Association between life-course models of neighbourhood deprivation, fractional anisotropy and mean diffusivity in 12 white matter tracts in Model 2

	Fractional anisotropy				Mean diffusivity			
	β	SE	p	p_{FDR}	β	SE	p	p_{FDR}
<i>Childhood neighbourhood deprivation (n=279 to 306)</i>								
Genu of corpus callosum	0.01	0.06	0.89	0.89	0.01	0.06	0.86	0.97
Splenium of corpus callosum	-0.07	0.06	0.21	0.66	0.09	0.06	0.12	0.84
Left arcuate fasciculus	-0.02	0.06	0.69	0.89	-0.01	0.06	0.81	0.97
Right arcuate fasciculus	-0.04	0.06	0.47	0.89	0.03	0.07	0.61	0.97
Left anterior thalamic radiation	-0.08	0.06	0.18	0.66	0.00	0.06	0.99	0.99
Right anterior thalamic radiation	0.01	0.06	0.86	0.89	-0.09	0.06	0.14	0.84
Left rostral cingulum	-0.10	0.06	0.10	0.66	0.03	0.06	0.64	0.97
Right rostral cingulum	-0.03	0.06	0.66	0.89	-0.01	0.06	0.89	0.97
Left inferior longitudinal fasciculus	0.03	0.06	0.61	0.89	-0.04	0.07	0.61	0.97
Right inferior longitudinal fasciculus	0.01	0.06	0.86	0.89	-0.07	0.06	0.23	0.90
Left uncinate fasciculus	-0.08	0.06	0.22	0.66	0.04	0.06	0.48	0.97
Right uncinate fasciculus	-0.03	0.06	0.63	0.89	0.03	0.06	0.67	0.97
<i>Young adulthood neighbourhood deprivation (n=346 to 375)</i>								
Genu of corpus callosum	-0.05	0.06	0.34	0.51	-0.05	0.06	0.39	0.73
Splenium of corpus callosum	-0.01	0.05	0.82	0.82	0.00	0.06	0.93	0.93
Left arcuate fasciculus	-0.10	0.05	0.07	0.27	-0.06	0.05	0.25	0.60
Right arcuate fasciculus	-0.04	0.06	0.43	0.57	-0.02	0.06	0.77	0.92
Left anterior thalamic radiation	-0.03	0.06	0.62	0.67	-0.12	0.06	0.03	0.39
Right anterior thalamic radiation	-0.04	0.06	0.48	0.58	-0.09	0.06	0.12	0.50
Left rostral cingulum	-0.06	0.06	0.29	0.50	-0.04	0.06	0.49	0.73
Right rostral cingulum	-0.07	0.05	0.17	0.35	-0.07	0.05	0.22	0.60
Left inferior longitudinal fasciculus	-0.08	0.06	0.15	0.35	0.11	0.07	0.11	0.50
Right inferior longitudinal fasciculus	-0.12	0.05	0.02	0.13	0.05	0.06	0.43	0.73
Left uncinate fasciculus	-0.14	0.06	0.01	0.13	-0.01	0.06	0.85	0.92
Right uncinate fasciculus	-0.09	0.06	0.09	0.27	0.02	0.06	0.78	0.92
<i>Mid- to late adulthood neighbourhood deprivation (n=359 to 387)</i>								
Genu of corpus callosum	-0.03	0.06	0.65	0.65	-0.03	0.06	0.57	0.74
Splenium of corpus callosum	-0.19	0.06	0.001	0.003	0.15	0.06	0.01	0.18
Left arcuate fasciculus	-0.16	0.05	0.004	0.01	0.08	0.06	0.14	0.41
Right arcuate fasciculus	-0.16	0.06	0.009	0.02	0.05	0.06	0.42	0.62
Left anterior thalamic radiation	-0.09	0.06	0.12	0.18	-0.07	0.06	0.22	0.44
Right anterior thalamic radiation	-0.19	0.06	0.001	0.003	0.12	0.06	0.04	0.24
Left rostral cingulum	-0.07	0.06	0.21	0.28	-0.01	0.06	0.84	0.84
Right rostral cingulum	-0.05	0.06	0.42	0.46	-0.02	0.06	0.75	0.82
Left inferior longitudinal fasciculus	-0.12	0.06	0.04	0.08	0.12	0.07	0.06	0.24
Right inferior longitudinal fasciculus	-0.18	0.06	0.001	0.003	0.08	0.06	0.19	0.44
Left uncinate fasciculus	-0.11	0.06	0.05	0.09	-0.05	0.06	0.38	0.62
Right uncinate fasciculus	-0.05	0.06	0.41	0.46	-0.03	0.06	0.62	0.74
<i>Accumulated neighbourhood deprivation (n=251 to 275)</i>								
Genu of corpus callosum	-0.02	0.07	0.82	0.95	-0.05	0.07	0.50	0.73
Splenium of corpus callosum	-0.18	0.07	0.01	0.10	0.17	0.07	0.02	0.20
Left arcuate fasciculus	-0.05	0.07	0.44	0.66	-0.04	0.07	0.55	0.73
Right arcuate fasciculus	-0.08	0.07	0.28	0.47	0.03	0.08	0.69	0.83
Left anterior thalamic radiation	-0.04	0.07	0.53	0.71	-0.14	0.07	0.05	0.30
Right anterior thalamic radiation	-0.11	0.07	0.10	0.28	-0.04	0.07	0.55	0.73
Left rostral cingulum	-0.12	0.07	0.09	0.28	-0.02	0.07	0.82	0.84
Right rostral cingulum	-0.01	0.07	0.87	0.95	-0.08	0.07	0.22	0.66
Left inferior longitudinal fasciculus	-0.10	0.07	0.16	0.32	0.14	0.08	0.10	0.42
Right inferior longitudinal fasciculus	-0.15	0.07	0.02	0.13	0.01	0.07	0.84	0.84
Left uncinate fasciculus	-0.12	0.08	0.12	0.28	-0.05	0.08	0.55	0.73
Right uncinate fasciculus	0.00	0.07	0.96	0.96	-0.07	0.08	0.35	0.73

Models were fitted within the structural equation modelling framework applying full information maximum likelihood estimation. Total sample size was $N=633$ for genu of corpus callosum, $N=652$ for splenium of corpus callosum, $N=655$ left arcuate fasciculus, and $N=621$ for right arcuate fasciculus, $N=643$ for left anterior thalamic radiation, $N=662$ right

anterior thalamic radiation, $N=647$ for left rostral cingulum, $N=643$ for right rostral cingulum, $N=663$ for left inferior longitudinal fasciculus, $N=663$ for left and right inferior longitudinal fasciculus, $N=618$ for left uncinate fasciculus and $N=647$ for right uncinate fasciculus; this table indicates ranges of observations for each exposure-outcomes pairs on which reported effect sizes are based (n). Bold typeface denotes false discovery rate adjusted significance (p_{FDR}). SE = standard error.

Models were adjusted for sex, age, father's occupational social class and *APOE* $\epsilon 4$ allele status. In addition, young adulthood models were adjusted for childhood IQ and years spent in education and mid- to late adulthood/ accumulation models also for adult occupational social class.

Supplementary Table 7: Interaction of neighbourhood deprivation with sex, *APOE* $\epsilon 4$ allele status and adult occupational social class and global brain outcomes

	Sex				<i>APOE</i> $\epsilon 4$ allele status				Father's social class				Adult social class			
	β	SE	<i>p</i>	<i>p</i> _{FDR}	β	SE	<i>p</i>	<i>p</i> _{FDR}	β	SE	<i>p</i>	<i>p</i> _{FDR}	β	SE	<i>p</i>	<i>p</i> _{FDR}
<i>Childhood neighbourhood deprivation (n=282 to 311)</i>																
Total brain volume	-0.05	0.07	0.43	0.85	-0.03	0.09	0.72	0.72	0.14	0.07	0.04	0.30	0.20	0.07	0.003	0.02
Grey matter volume	-0.05	0.10	0.59	0.85	-0.08	0.14	0.56	0.72	0.04	0.10	0.72	0.80	0.24	0.10	0.02	0.049
Normal-appearing white matter volume	-0.03	0.10	0.74	0.85	0.15	0.13	0.25	0.72	0.07	0.10	0.53	0.80	0.07	0.11	0.49	0.79
White matter hyperintensity volume	0.10	0.16	0.51	0.85	-0.22	0.22	0.32	0.72	0.11	0.16	0.51	0.80	-0.02	0.17	0.92	0.92
Cortical surface area	0.01	0.09	0.94	0.94	-0.06	0.13	0.65	0.72	0.10	0.10	0.34	0.80	0.13	0.10	0.21	0.41
Mean cortical thickness	0.09	0.18	0.61	0.85	-0.10	0.25	0.69	0.72	0.05	0.19	0.80	0.80	0.06	0.20	0.76	0.87
General fractional anisotropy ^a	0.12	0.19	0.50	0.85	-0.11	0.26	0.67	0.72	0.23	0.19	0.23	0.80	0.52	0.20	0.009	0.04
General mean diffusivity ^a	-0.09	0.19	0.65	0.85	0.39	0.26	0.14	0.72	0.09	0.20	0.66	0.80	0.07	0.21	0.74	0.87
<i>Young adulthood neighbourhood deprivation (n=348 to 383)</i>																
Total brain volume	-0.07	0.06	0.24	0.83	-0.03	0.07	0.72	0.99	0.16	0.06	0.01	0.05	0.20	0.06	0.002	0.007
Grey matter volume	0.03	0.09	0.73	0.83	0.07	0.11	0.50	0.99	0.09	0.09	0.36	0.58	0.34	0.09	<0.001	0.001
Normal-appearing white matter volume	-0.15	0.09	0.10	0.81	0.00	0.12	0.98	0.99	0.11	0.10	0.29	0.58	-0.02	0.10	0.86	0.86
White matter hyperintensity volume	0.13	0.14	0.36	0.83	-0.44	0.17	0.01	0.09	0.06	0.15	0.66	0.75	0.17	0.15	0.26	0.35
Cortical surface area	0.00	0.08	0.97	0.97	-0.18	0.10	0.08	0.32	0.24	0.09	0.005	0.04	0.11	0.09	0.22	0.35
Mean cortical thickness	0.06	0.16	0.69	0.83	0.29	0.20	0.14	0.37	-0.12	0.16	0.48	0.64	0.39	0.17	0.02	0.06
General fractional anisotropy ^a	0.10	0.17	0.57	0.83	-0.06	0.21	0.77	0.99	0.32	0.18	0.07	0.17	0.35	0.18	0.06	0.11
General mean diffusivity ^a	0.10	0.17	0.58	0.83	0.00	0.22	0.99	0.99	0.02	0.18	0.92	0.92	0.09	0.19	0.64	0.73
<i>Mid- to late adulthood neighbourhood deprivation (n=359 to 396)</i>																
Total brain volume	0.01	0.06	0.90	0.97	-0.09	0.07	0.22	0.52	0.05	0.07	0.50	0.72	0.10	0.07	0.12	0.31
Grey matter volume	0.09	0.09	0.31	0.82	0.08	0.11	0.46	0.52	-0.01	0.10	0.89	0.89	0.25	0.10	0.01	0.08
Normal-appearing white matter volume	-0.10	0.09	0.26	0.82	-0.07	0.11	0.55	0.55	0.06	0.10	0.54	0.72	-0.17	0.10	0.09	0.31
White matter hyperintensity volume	0.09	0.14	0.50	0.97	-0.39	0.17	0.02	0.17	0.28	0.15	0.07	0.26	0.14	0.16	0.35	0.47
Cortical surface area	0.02	0.08	0.77	0.97	-0.08	0.10	0.44	0.52	0.23	0.09	0.01	0.06	0.00	0.09	0.98	0.98
Mean cortical thickness	0.01	0.16	0.97	0.97	-0.17	0.20	0.38	0.52	-0.18	0.17	0.30	0.60	0.10	0.18	0.57	0.65
General fractional anisotropy ^a	-0.06	0.17	0.71	0.97	-0.20	0.20	0.32	0.52	0.22	0.18	0.22	0.60	-0.24	0.19	0.19	0.39
General mean diffusivity ^a	0.20	0.17	0.25	0.82	-0.18	0.21	0.41	0.52	0.06	0.19	0.73	0.84	0.21	0.19	0.28	0.44
<i>Accumulated neighbourhood deprivation (n=255 to 281)</i>																
Total brain volume	-0.04	0.07	0.52	0.93	-0.10	0.09	0.30	0.57	0.15	0.08	0.04	0.17	0.21	0.07	0.003	0.01
Grey matter volume	-0.01	0.10	0.96	0.96	-0.11	0.15	0.43	0.57	0.12	0.12	0.30	0.50	0.31	0.11	0.003	0.01
Normal-appearing white matter volume	-0.05	0.10	0.62	0.93	0.12	0.15	0.40	0.57	0.12	0.12	0.31	0.50	-0.01	0.11	0.93	0.93
White matter hyperintensity volume	0.08	0.16	0.63	0.93	-0.44	0.22	0.05	0.36	0.15	0.18	0.41	0.54	0.17	0.17	0.34	0.55
Cortical surface area	0.04	0.10	0.67	0.93	-0.18	0.13	0.18	0.57	0.24	0.10	0.02	0.17	0.17	0.10	0.10	0.28
Mean cortical thickness	0.07	0.19	0.73	0.93	-0.18	0.28	0.51	0.58	-0.07	0.21	0.76	0.82	0.15	0.21	0.46	0.62
General fractional anisotropy ^a	0.23	0.20	0.25	0.93	-0.04	0.27	0.89	0.89	0.40	0.21	0.06	0.17	0.30	0.21	0.16	0.33
General mean diffusivity ^a	-0.05	0.21	0.82	0.93	0.27	0.29	0.36	0.57	0.05	0.23	0.82	0.82	0.10	0.23	0.65	0.77

Models with relevant interaction terms were fitted within the structural equation modelling framework applying full information maximum likelihood estimation. Total sample size was $N=658$ for total brain, grey matter and normal-appearing white matter volumes, $N=672$ for white matter hyperintensity volume, $N=636$ for cortical surface area and mean cortical thickness, and $N=665$ for general fractional anisotropy and mean diffusivity; this table indicates ranges of observations for each exposure-outcomes pairs on which reported effect sizes are based (n). Bold typeface denotes false discovery rate adjusted significance (p_{FDR}). SE = standard error.

Models were adjusted for sex, age, (intracranial volume for macrostructural measures,) father's occupational social class and APOE $\epsilon 4$ allele status. In addition, young adulthood models were adjusted for childhood IQ and years spent in education, and mid- to late adulthood/ accumulation models also for adult occupational social class.

^aNo adjustment for intracranial volume.

Supplementary Table 8: Association between life-course models of neighbourhood deprivation and global brain outcomes stratified by adult occupational social class

	High: Professional-managerial				Low: Skilled, partly skilled, and unskilled			
	β	SE	<i>p</i>	<i>p</i> _{FDR}	β	SE	<i>p</i>	<i>p</i> _{FDR}
<i>Childhood neighbourhood deprivation</i>	(n=168 to 173)				(n=126 to 136)			
Total brain volume	0.02	0.03	0.39	0.77	-0.10	0.03	0.003	0.01
Grey matter volume	0.01	0.04	0.76	0.88	-0.12	0.05	0.02	0.05
Normal-appearing white matter volume	0.04	0.04	0.35	0.77	-0.02	0.05	0.76	0.90
White matter hyperintensity volume	-0.02	0.07	0.77	0.88	-0.02	0.08	0.83	0.90
Cortical surface area	0.04	0.04	0.33	0.77	-0.04	0.05	0.36	0.63
Mean cortical thickness	-0.05	0.08	0.51	0.82	-0.08	0.09	0.39	0.63
General fractional anisotropy ^a	0.08	0.08	0.33	0.77	-0.26	0.09	0.003	0.01
General mean diffusivity ^a	0.00	0.08	0.99	0.99	0.01	0.10	0.90	0.90
<i>Young adulthood neighbourhood deprivation</i>	(n=220 to 226)				(n=144 to 154)			
Total brain volume	0.03	0.03	0.17	0.78	-0.08	0.03	0.013	0.03
Grey matter volume	0.04	0.04	0.29	0.78	-0.15	0.05	0.002	0.005
Normal-appearing white matter volume	0.05	0.04	0.24	0.78	0.05	0.05	0.27	0.31
White matter hyperintensity volume	0.03	0.06	0.62	0.85	-0.11	0.08	0.14	0.19
Cortical surface area	-0.01	0.04	0.74	0.85	-0.09	0.05	0.05	0.08
Mean cortical thickness	-0.01	0.07	0.87	0.87	-0.25	0.08	0.002	0.005
General fractional anisotropy ^a	-0.03	0.08	0.66	0.85	-0.28	0.08	0.001	0.005
General mean diffusivity ^a	-0.04	0.08	0.56	0.85	-0.04	0.10	0.65	0.65
<i>Mid- to late adulthood neighbourhood deprivation</i>	(n=233 to 240)				(n=144 to 154)			
Total brain volume	-0.03	0.03	0.19	0.31	-0.09	0.03	0.006	0.022
Grey matter volume	-0.04	0.04	0.26	0.32	-0.18	0.05	<0.001	0.003
Normal-appearing white matter volume	-0.11	0.04	0.004	0.017	-0.04	0.05	0.45	0.62
White matter hyperintensity volume	0.10	0.07	0.14	0.27	-0.01	0.08	0.94	0.94
Cortical surface area	-0.04	0.04	0.32	0.32	-0.04	0.05	0.46	0.62
Mean cortical thickness	-0.13	0.07	0.08	0.22	-0.19	0.09	0.03	0.09
General fractional anisotropy ^a	-0.26	0.07	<0.001	0.003	-0.12	0.09	0.19	0.38
General mean diffusivity ^a	0.08	0.08	0.32	0.32	-0.02	0.10	0.85	0.94
<i>Accumulated neighbourhood deprivation</i>	(n=147 to 151)				(n=120 to 129)			
Total brain volume	0.02	0.03	0.44	0.87	-0.13	0.04	<0.001	0.001
Grey matter volume	0.01	0.05	0.76	0.87	-0.21	0.06	<0.001	0.001
Normal-appearing white matter volume	0.02	0.05	0.69	0.87	0.01	0.05	0.79	0.85
White matter hyperintensity volume	0.05	0.08	0.56	0.87	-0.09	0.09	0.29	0.39
Cortical surface area	0.04	0.05	0.36	0.87	-0.09	0.05	0.10	0.15
Mean cortical thickness	-0.04	0.10	0.67	0.87	-0.19	0.10	0.06	0.13
General fractional anisotropy ^a	0.00	0.10	0.97	0.97	-0.27	0.10	0.006	0.016
General mean diffusivity ^a	-0.08	0.10	0.43	0.87	-0.02	0.11	0.85	0.85

Models were fitted within the structural equation modelling framework applying full information maximum likelihood estimation. Total sample size was $N=376/N=272$ for total brain, grey matter and normal-appearing white matter volume, $N=383/N=278$ for white matter hyperintensity volume, $N=368/N=257$ for cortical surface area and mean cortical thickness, and $N=381/274$ for general fractional anisotropy and mean diffusivity among high/low social classes; this table indicates ranges of observations for exposure-outcomes pairs (*n*). Bold typeface denotes false discovery rate adjusted significance (*p*_{FDR}). SE = standard error.

Models were adjusted for sex, age, (intracranial volume for macrostructural measures,) father's occupational social class and *APOE* ε4 allele status. In addition, young adulthood models were adjusted for childhood IQ and years spent in education, and mid- to late adulthood/ accumulation models also for adult occupational social class.

^aNo adjustment for intracranial volume

Supplementary Table 9: Association between life-course models of neighbourhood deprivation and global brain outcomes after considering exposure during previous epoch

	Model 2 – S1				% Change from Model 2 ^a
	β	SE	p	p_{FDR}	
<i>Young adulthood neighbourhood deprivation (n=367 to 383)</i>					
Total brain volume	0.01	0.02	0.69	0.78	-150.00%
Grey matter volume	-0.03	0.04	0.47	0.63	-40.00%
Normal-appearing white matter volume	0.07	0.04	0.08	0.21	40.00%
White matter hyperintensity volume	-0.02	0.06	0.78	0.78	-55.00%
Cortical surface area	-0.05	0.04	0.15	0.30	0.00%
Mean cortical thickness	-0.12	0.07	0.07	0.21	-20.00%
General fractional anisotropy ^b	-0.13	0.07	0.06	0.21	-7.14%
General mean diffusivity ^b	-0.09	0.07	0.22	0.35	50.00%
<i>Mid- to late adulthood neighbourhood deprivation (n=379 to 396)</i>					
Total brain volume	-0.05	0.02	0.03	0.04	-16.67%
Grey matter volume	-0.09	0.03	0.01	0.03	-18.18%
Normal-appearing white matter volume	-0.09	0.03	0.01	0.03	28.57%
White matter hyperintensity volume	0.07	0.05	0.22	0.29	40.00%
Cortical surface area	-0.01	0.03	0.67	0.76	-75.00%
Mean cortical thickness	-0.15	0.06	0.02	0.03	0.00%
General fractional anisotropy ^b	-0.17	0.06	0.01	0.03	-10.53%
General mean diffusivity ^b	0.01	0.07	0.86	0.86	-66.67%

Models were fitted within the structural equation modelling framework applying full information maximum likelihood estimation; exposure of interest was regressed on exposure during the previous period (i.e., young adulthood on childhood, mid- to late adulthood on young adulthood neighbourhood deprivation). Models for childhood neighbourhood deprivation and accumulated neighbourhood deprivation are not presented as this sensitivity analysis cannot be applied for them. Total sample size was $N=658$ for total brain, grey matter and normal-appearing white matter volumes, $N=672$ for white matter hyperintensity volume, $N=636$ for cortical surface area and mean cortical thickness, and $N=665$ for general fractional anisotropy and mean diffusivity; this table indicates ranges of observations for each exposure-outcomes pairs on which reported effect sizes are based (n). Bold typeface denotes false discovery rate adjusted significance (p_{FDR}). SE = standard error.

Models were adjusted for sex, age, (intracranial volume for macrostructural measures,) father's occupational social class, *APOE* $\epsilon 4$ allele status, childhood IQ, years spent in education and neighbourhood deprivation during previous exposure period, mid- to late adulthood models also adjusted for adult occupational social class.

^a Main models did not include neighbourhood deprivation in previous epochs.

^b No adjustment for intracranial volume.

Supplementary Table 10: Association between life-course models of neighbourhood deprivation and global brain outcomes after adjusting for stroke identified from MRI scans

	Model 2 – S2			
	β	SE	p	p_{FDR}
<i>Childhood neighbourhood deprivation (n=296 to 311)</i>				
Total brain volume	-0.04	0.02	0.10	0.39
Grey matter volume	-0.05	0.03	0.09	0.39
Normal-appearing white matter volume	0.02	0.03	0.58	0.77
White matter hyperintensity volume	-0.03	0.05	0.57	0.77
Cortical surface area	-0.01	0.03	0.84	0.96
Mean cortical thickness	-0.07	0.06	0.23	0.61
General fractional anisotropy ^a	-0.06	0.06	0.30	0.61
General mean diffusivity ^a	0.00	0.06	0.98	0.98
<i>Young adulthood neighbourhood social deprivation (n=367 to 383)</i>				
Total brain volume	-0.02	0.02	0.34	0.44
Grey matter volume	-0.05	0.03	0.11	0.22
Normal-appearing white matter volume	0.05	0.03	0.14	0.22
White matter hyperintensity volume	-0.03	0.05	0.48	0.48
Cortical surface area	-0.05	0.03	0.06	0.17
Mean cortical thickness	-0.10	0.05	0.06	0.17
General fractional anisotropy ^a	-0.14	0.06	0.01	0.11
General mean diffusivity ^a	-0.05	0.06	0.39	0.44
<i>Mid- to late adulthood neighbourhood deprivation (n=379 to 396)</i>				
Total brain volume	-0.06	0.02	0.01	0.02
Grey matter volume	-0.10	0.03	0.002	0.009
Normal-appearing white matter volume	-0.06	0.03	0.07	0.11
White matter hyperintensity volume	0.04	0.05	0.46	0.52
Cortical surface area	-0.04	0.03	0.16	0.21
Mean cortical thickness	-0.15	0.06	0.01	0.02
General fractional anisotropy ^a	-0.18	0.06	0.002	0.009
General mean diffusivity ^a	0.01	0.06	0.83	0.83
<i>Accumulated neighbourhood deprivation (n=268 to 281)</i>				
Total brain volume	-0.05	0.03	0.05	0.20
Grey matter volume	-0.09	0.04	0.02	0.19
Normal-appearing white matter volume	0.02	0.04	0.53	0.57
White matter hyperintensity volume	-0.03	0.06	0.57	0.57
Cortical surface area	-0.02	0.04	0.53	0.57
Mean cortical thickness	-0.11	0.07	0.15	0.29
General fractional anisotropy ^a	-0.13	0.07	0.08	0.22
General mean diffusivity ^a	-0.07	0.08	0.38	0.57

Models were fitted within the structural equation modelling framework applying full information maximum likelihood estimation. Total sample size was N=658 for total brain, grey matter and normal-appearing white matter volume, N=672 for white matter hyperintensity volume, N=636 for cortical surface area and mean cortical thickness, and N=665 for general fractional anisotropy and mean diffusivity; this table indicates ranges of observations for each exposure-outcomes pairs on which reported effect sizes are based (n). Bold typeface denotes false discovery rate adjusted significance (p_{FDR}). SE = standard error.

Models were adjusted for sex, age, MRI-based stroke, (intracranial volume for macrostructural measures,) father's occupational social class and *APOE* $\epsilon 4$ allele status. In addition, young adulthood models were adjusted for childhood IQ and years spent in education, and mid- to late adulthood / accumulation models also for adult occupational social class.

^a No adjustment for intracranial volume

Supplementary Table 11: Association between mid-to-late adulthood neighbourhood deprivation and global brain outcomes after adjusting for late adulthood health status

	Model 2 – S3				% Change from Model 2 ^a
	β	SE	p	p_{FDR}	
<i>Mid- to late adulthood neighbourhood deprivation (n=379 to 396)</i>					
Total brain volume	-0.05	0.02	0.02	0.05	-16.67%
Grey matter volume	-0.09	0.03	0.004	0.02	-18.18%
Normal-appearing white matter volume	-0.05	0.03	0.10	0.15	-28.57%
White matter hyperintensity volume	0.04	0.05	0.42	0.48	-20.00%
Cortical surface area	-0.04	0.03	0.20	0.27	0.00%
Mean cortical thickness	-0.10	0.06	0.07	0.15	-33.33%
General fractional anisotropy ^b	-0.17	0.06	0.004	0.02	-10.53%
General mean diffusivity ^b	0.02	0.06	0.71	0.71	-33.33%

Models were fitted within the structural equation modelling framework applying full information maximum likelihood estimation. Total sample size was $N=658$ for total brain, grey matter and normal-appearing white matter volumes, $N=672$ for white matter hyperintensity volume, $N=636$ for cortical surface area and mean cortical thickness, and $N=665$ for general fractional anisotropy and mean diffusivity; this table indicates ranges of observations for each exposure-outcomes pairs on which reported effect sizes are based (n). Bold typeface denotes false discovery rate adjusted significance (p_{FDR}). SE = standard error.

Models were adjusted for sex, age, (intracranial volume for volumetric measures,) father's occupational social class, *APOE* $\epsilon 4$ allele status, childhood IQ, years spent in education, adult occupational social class, smoking status, BMI, and history of hypertension, diabetes, stroke, and cardiovascular diseases.

^a Main models did not include health-related variables.

^b No adjustment for intracranial volume

Supplementary Table 12: Association between life-course models of neighbourhood deprivation and global brain outcomes among those living in Edinburgh throughout each decade of the exposure periods

	Model 2 – S4			
	β	SE	p	p_{FDR}
<i>Childhood neighbourhood social deprivation (n=264 to 276)</i>				
Total brain volume	-0.06	0.02	0.02	0.17
Grey matter volume	-0.06	0.04	0.10	0.39
Normal-appearing white matter volume	0.00	0.04	0.92	0.92
White matter hyperintensity volume	-0.03	0.06	0.64	0.85
Cortical surface area	-0.02	0.03	0.59	0.85
Mean cortical thickness	-0.07	0.07	0.32	0.64
General fractional anisotropy ^a	-0.08	0.07	0.25	0.64
General mean diffusivity ^a	-0.02	0.07	0.81	0.92
<i>Young adulthood neighbourhood social deprivation (n=300 to 314)</i>				
Total brain volume	-0.02	0.02	0.46	0.52
Grey matter volume	-0.03	0.04	0.46	0.52
Normal-appearing white matter volume	0.05	0.04	0.16	0.42
White matter hyperintensity volume	-0.05	0.05	0.39	0.52
Cortical surface area	-0.06	0.03	0.07	0.28
Mean cortical thickness	-0.02	0.07	0.72	0.72
General fractional anisotropy ^a	-0.12	0.07	0.06	0.28
General mean diffusivity ^a	-0.08	0.07	0.24	0.48
<i>Mid- to late adulthood neighbourhood deprivation (n=333 to 350)</i>				
Total brain volume	-0.06	0.02	0.02	0.05
Grey matter volume	-0.10	0.03	0.004	0.03
Normal-appearing white matter volume	-0.06	0.03	0.07	0.12
White matter hyperintensity volume	0.04	0.05	0.48	0.48
Cortical surface area	-0.03	0.03	0.45	0.48
Mean cortical thickness	-0.16	0.06	0.01	0.04
General fractional anisotropy ^a	-0.15	0.07	0.02	0.05
General mean diffusivity ^a	-0.05	0.07	0.46	0.48
<i>Accumulated neighbourhood deprivation (n=216 to 226)</i>				
Total brain volume	-0.09	0.03	0.004	0.03
Grey matter volume	-0.12	0.05	0.01	0.05
Normal-appearing white matter volume	-0.01	0.05	0.88	0.88
White matter hyperintensity volume	-0.03	0.07	0.66	0.75
Cortical surface area	-0.04	0.04	0.34	0.45
Mean cortical thickness	-0.12	0.09	0.17	0.34
General fractional anisotropy ^a	-0.16	0.09	0.08	0.20
General mean diffusivity ^a	-0.09	0.10	0.33	0.45

Models were fitted within the structural equation modelling framework applying full information maximum likelihood estimation. Total sample size was $N=658$ for total brain, grey matter and normal-appearing white matter volumes, $N=672$ for white matter hyperintensity volume, $N=636$ for cortical surface area and mean cortical thickness, and $N=665$ for general fractional anisotropy and mean diffusivity; this table indicates ranges of observations for each exposure-outcomes pairs on which reported effect sizes are based (n). Bold typeface denotes false discovery rate adjusted significance (p_{FDR}). SE = standard error.

Models were adjusted for sex, age, (intracranial volume for macrostructural measures,) father's occupational social class and *APOE* $\epsilon 4$ allele status. In addition, young adulthood models were adjusted for childhood IQ and years spent in education, and mid- to late adulthood/ accumulation models also for adult occupational social class.

^a No adjustment for intracranial volume

Supplementary Table 13: Association between life-course models of neighbourhood deprivation and global brain outcomes among individuals without cognitive impairment

	Model 2 – S5			
	β	SE	p	p_{FDR}
<i>Childhood neighbourhood social deprivation (n=246 to 255)</i>				
Total brain volume	-0.05	0.02	0.01	0.10
Grey matter volume	-0.05	0.03	0.11	0.44
Normal-appearing white matter volume	0.00	0.03	1.00	1.00
White matter hyperintensity volume	-0.05	0.05	0.34	0.54
Cortical surface area	-0.01	0.03	0.70	0.80
Mean cortical thickness	-0.08	0.06	0.20	0.53
General fractional anisotropy ^a	-0.07	0.07	0.30	0.54
General mean diffusivity ^a	-0.03	0.07	0.61	0.80
<i>Young adulthood neighbourhood social deprivation (n=280 to 292)</i>				
Total brain volume	-0.03	0.02	0.22	0.28
Grey matter volume	-0.04	0.03	0.21	0.28
Normal-appearing white matter volume	0.04	0.03	0.24	0.28
White matter hyperintensity volume	-0.05	0.05	0.31	0.31
Cortical surface area	-0.06	0.03	0.04	0.15
Mean cortical thickness	-0.10	0.06	0.06	0.17
General fractional anisotropy ^a	-0.17	0.06	0.005	0.04
General mean diffusivity ^a	-0.09	0.06	0.17	0.28
<i>Mid- to late adulthood neighbourhood deprivation (n=313 to 328)</i>				
Total brain volume	-0.07	0.02	0.003	0.01
Grey matter volume	-0.11	0.03	0.001	0.008
Normal-appearing white matter volume	-0.09	0.03	0.006	0.01
White matter hyperintensity volume	0.05	0.05	0.39	0.44
Cortical surface area	-0.04	0.03	0.18	0.23
Mean cortical thickness	-0.15	0.06	0.009	0.01
General fractional anisotropy ^a	-0.18	0.06	0.004	0.01
General mean diffusivity ^a	0.03	0.07	0.69	0.69
<i>Accumulated neighbourhood deprivation (n=201 to 209)</i>				
Total brain volume	-0.07	0.03	0.006	0.047
Grey matter volume	-0.09	0.04	0.02	0.10
Normal-appearing white matter volume	-0.02	0.04	0.61	0.61
White matter hyperintensity volume	-0.04	0.06	0.50	0.58
Cortical surface area	-0.03	0.04	0.37	0.51
Mean cortical thickness	-0.12	0.08	0.13	0.26
General fractional anisotropy ^a	-0.15	0.08	0.06	0.15
General mean diffusivity ^a	-0.07	0.08	0.39	0.51

Models were fitted within the structural equation modelling framework applying full information maximum likelihood estimation. Cognitive impairment was defined as either having a diagnosis of dementia or scoring <24 points in the Mini Mental State Examination. Total sample size was $N=611$ for total brain, grey matter and normal-appearing white matter volume, $N=625$ for white matter hyperintensity volume, $N=594$ for cortical surface area and mean cortical thickness, and $N=620$ for general fractional anisotropy and mean diffusivity; ranges of observations for exposure-outcomes pairs are presented in the table (n). Bold typeface denotes false discovery rate adjusted significance (p_{FDR}). SE = standard error.

Models were adjusted for sex, age, (intracranial volume for macrostructural measures,) father's occupational social class and *APOE* $\epsilon 4$ allele status. In addition, young adulthood models were adjusted for childhood IQ and years spent in education, and mid- to late adulthood/ accumulation models also for adult occupational social class.

^a No adjustment for intracranial volume

Supplementary Table 14: Complete case analysis testing the association between life-course models of neighbourhood deprivation and global brain outcomes

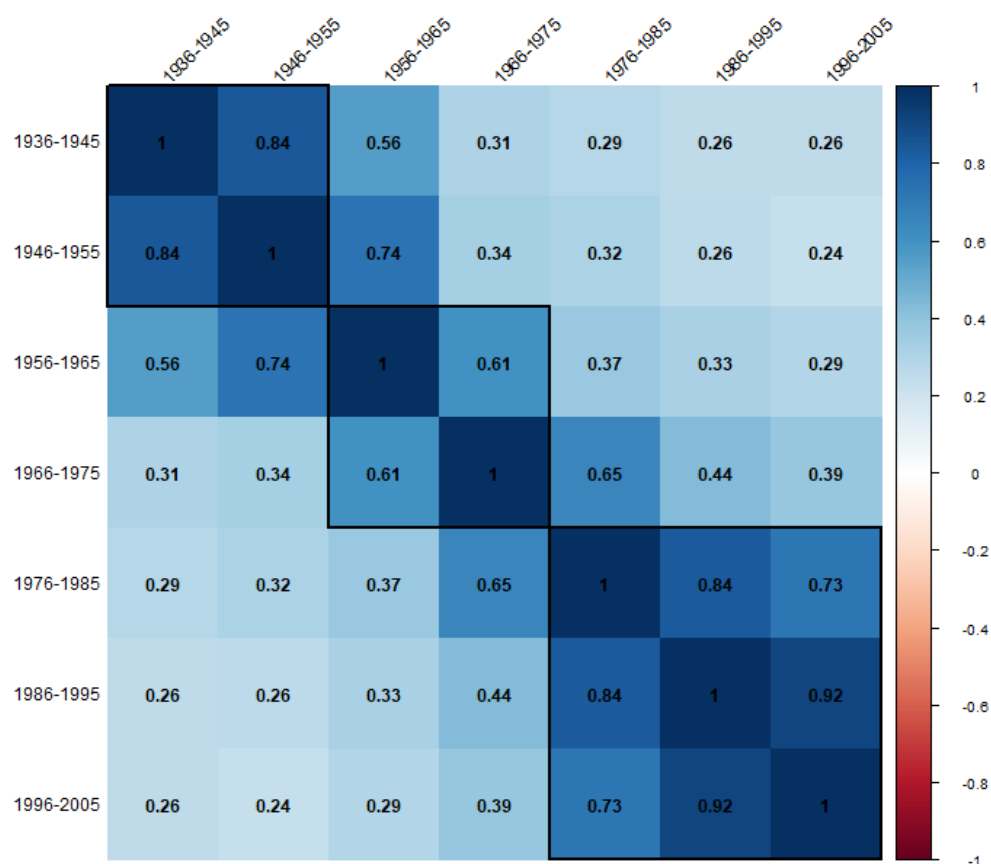
	Model 2 – S6			
	β	SE	p	p_{FDR}
<i>Childhood neighbourhood deprivation</i>				
Total brain volume ($N=261$)	-0.05	0.02	0.02	0.13
Grey matter volume ($N=261$)	-0.05	0.04	0.16	0.54
Normal-appearing white matter volume ($N=261$)	0.00	0.03	0.94	0.94
White matter hyperintensity volume ($N=266$)	-0.06	0.07	0.40	0.64
Cortical surface area ($N=255$)	-0.02	0.04	0.64	0.86
Mean cortical thickness ($N=255$)	-0.07	0.07	0.27	0.54
General fractional anisotropy ^a ($N=263$)	-0.08	0.07	0.25	0.54
General mean diffusivity ^a ($N=263$)	-0.02	0.06	0.81	0.92
<i>Young adulthood neighbourhood deprivation</i>				
Total brain volume ($N=310$)	-0.02	0.02	0.27	0.44
Grey matter volume ($N=310$)	-0.03	0.03	0.39	0.46
Normal-appearing white matter volume ($N=310$)	0.02	0.03	0.46	0.46
White matter hyperintensity volume ($N=316$)	-0.07	0.07	0.28	0.44
Cortical surface area ($N=304$)	-0.08	0.03	0.02	0.09
Mean cortical thickness ($N=304$)	-0.09	0.06	0.17	0.44
General fractional anisotropy ^a ($N=311$)	-0.18	0.06	0.005	0.04
General mean diffusivity ^a ($N=311$)	-0.05	0.06	0.41	0.46
<i>Mid- to late adulthood neighbourhood deprivation</i>				
Total brain volume ($N=321$)	-0.05	0.02	0.03	0.07
Grey matter volume ($N=321$)	-0.07	0.03	0.04	0.08
Normal-appearing white matter volume ($N=321$)	-0.07	0.03	0.01	0.06
White matter hyperintensity volume ($N=326$)	0.03	0.07	0.67	0.68
Cortical surface area ($N=313$)	-0.04	0.04	0.33	0.45
Mean cortical thickness ($N=313$)	-0.13	0.07	0.06	0.09
General fractional anisotropy ^a ($N=321$)	-0.20	0.06	0.002	0.02
General mean diffusivity ^a ($N=321$)	0.03	0.06	0.68	0.68
<i>Accumulated neighbourhood deprivation</i>				
Total brain volume ($N=228$)	-0.06	0.03	0.02	0.18
Grey matter volume ($N=228$)	-0.06	0.04	0.11	0.29
Normal-appearing white matter volume ($N=228$)	-0.01	0.04	0.70	0.70
White matter hyperintensity volume ($N=232$)	-0.06	0.09	0.52	0.60
Cortical surface area ($N=222$)	-0.04	0.04	0.36	0.49
Mean cortical thickness ($N=222$)	-0.07	0.08	0.37	0.49
General fractional anisotropy ^a ($N=229$)	-0.15	0.08	0.06	0.23
General mean diffusivity ^a ($N=229$)	-0.07	0.06	0.30	0.49

Models were fitted with multivariate linear regression applying complete case analysis; therefore, underlying sample sizes differ across the presented estimates. Latent factors of general fractional anisotropy and general mean diffusivity were predicted and extracted from the measurement model. Sample sizes for each model are indicated in the table (N). Bold typeface denotes false discovery rate adjusted significance (p_{FDR}). SE = standard error.

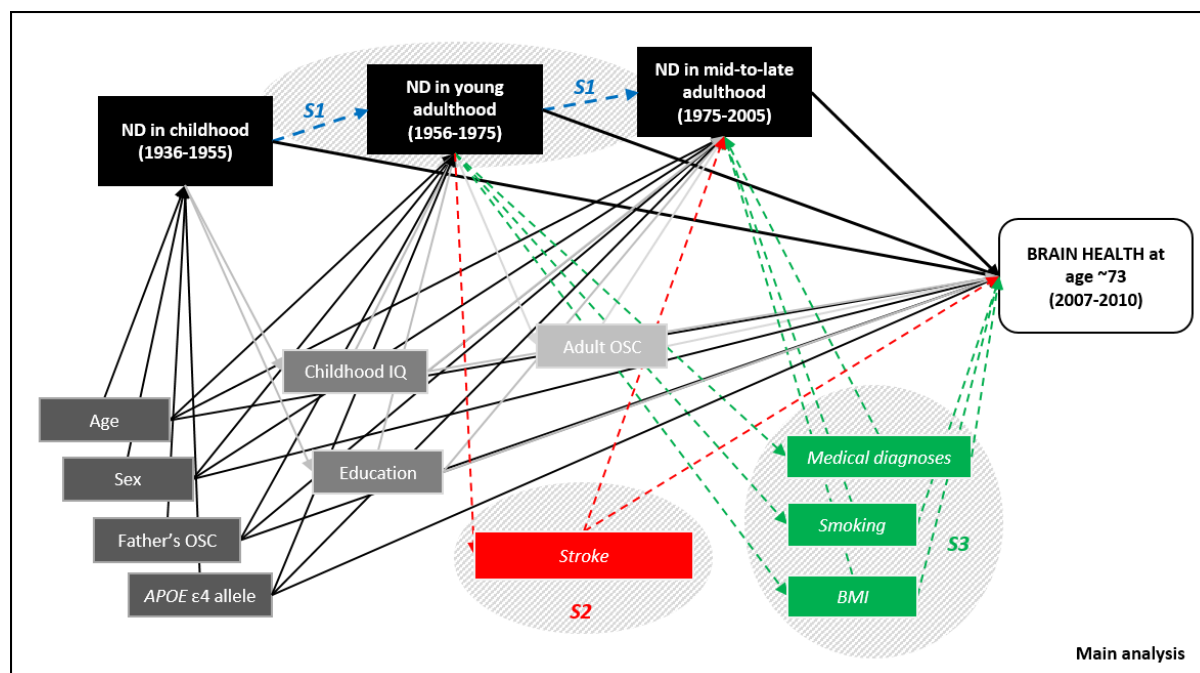
Models were adjusted for sex, age, (intracranial volume for macrostructural measures,) father's occupational social class and *APOE* $\epsilon 4$ allele status. In addition, young adulthood models were adjusted for childhood IQ and years spent in education, and mid- to late adulthood/ accumulation models also for adult occupational social class.

^a No adjustment for intracranial volume

Supplementary Figure 8: Pearson's correlation coefficients between individual exposures to neighbourhood deprivation. Pairwise deletion was applied for missing values to preserve the maximum amount of information. Black rectangles indicate childhood (1936-1955), young adulthood (1956-1975), and mid- to late adulthood (1976-2005) periods. All presented correlation coefficients were significant ($p < 0.001$).



Supplementary Figure 9: Directed acyclic graph representing associations between neighbourhood deprivation, global brain outcomes and confounders considered in the main and sensitivity analyses. Confounders included in the main analyses are coloured grey: dark grey are considered as confounders for all life course models, medium grey for young adulthood and mid- to late adulthood exposures, light grey for mid- to late adulthood exposures only. Sensitivity analyses considering selective mobility (S1) and potential health-related confounders (S2, S3) are blue, red, and green, respectively. Links between confounders are not shown for simplicity. BMI = body mass index; IQ = intelligence quotient; ND = neighbourhood deprivation; OSC = occupational social class.



Supplementary Table 15: Standardized tract loadings, explained variance and goodness of fit indices for fractional anisotropy and mean diffusivity

	Fractional anisotropy	Mean diffusivity
<i>Standardized tract loadings</i>		
Genu of corpus callosum	0.57	0.57
Splenium of corpus callosum	0.41	0.28
Left arcuate fasciculus	0.65	0.70
Right arcuate fasciculus	0.65	0.74
Left anterior thalamic radiation	0.62	0.67
Right anterior thalamic radiation	0.60	0.58
Left rostral cingulum	0.52	0.60
Right rostral cingulum	0.53	0.72
Left inferior longitudinal fasciculus	0.46	0.37
Right inferior longitudinal fasciculus	0.44	0.36
Left uncinate fasciculus	0.62	0.63
Right uncinate fasciculus	0.65	0.68
<i>% of variance explained</i>		
	32.0%	35.2%
<i>Goodness of fit indices</i>		
Comparative Fit Index	0.97	0.97
Tucker Lewis Index	0.96	0.96
Root Mean Square Error of Approximation	0.04	0.05
Standardised Root Mean Square Residual	0.03	0.03
Chi-squared ₍₄₈₎	106.34	131.43
<i>p</i> -value	<0.001	<0.001

Reference values are: Comparative Fit Index>0.95; Tucker-Lewis Index>0.95; Root Mean Square Error of Approximation<0.06; and Standardized Root Mean Square Residual<0.08 (1).

References

1. Hu Lt, Bentler PM. Cutoff criteria for fit indexes in covariance structure analysis: Conventional criteria versus new alternatives. *Structural Equation Modeling: A Multidisciplinary Journal*. 1999;6(1):1-55.
2. Lyall DM, Harris SE, Bastin ME, Muñoz Maniega S, Murray C, Lutz MW, et al. Alzheimer's disease susceptibility genes APOE and TOMM40, and brain white matter integrity in the Lothian Birth Cohort 1936. *Neurobiol Aging*. 2014;35(6):1513.e25-.e33.